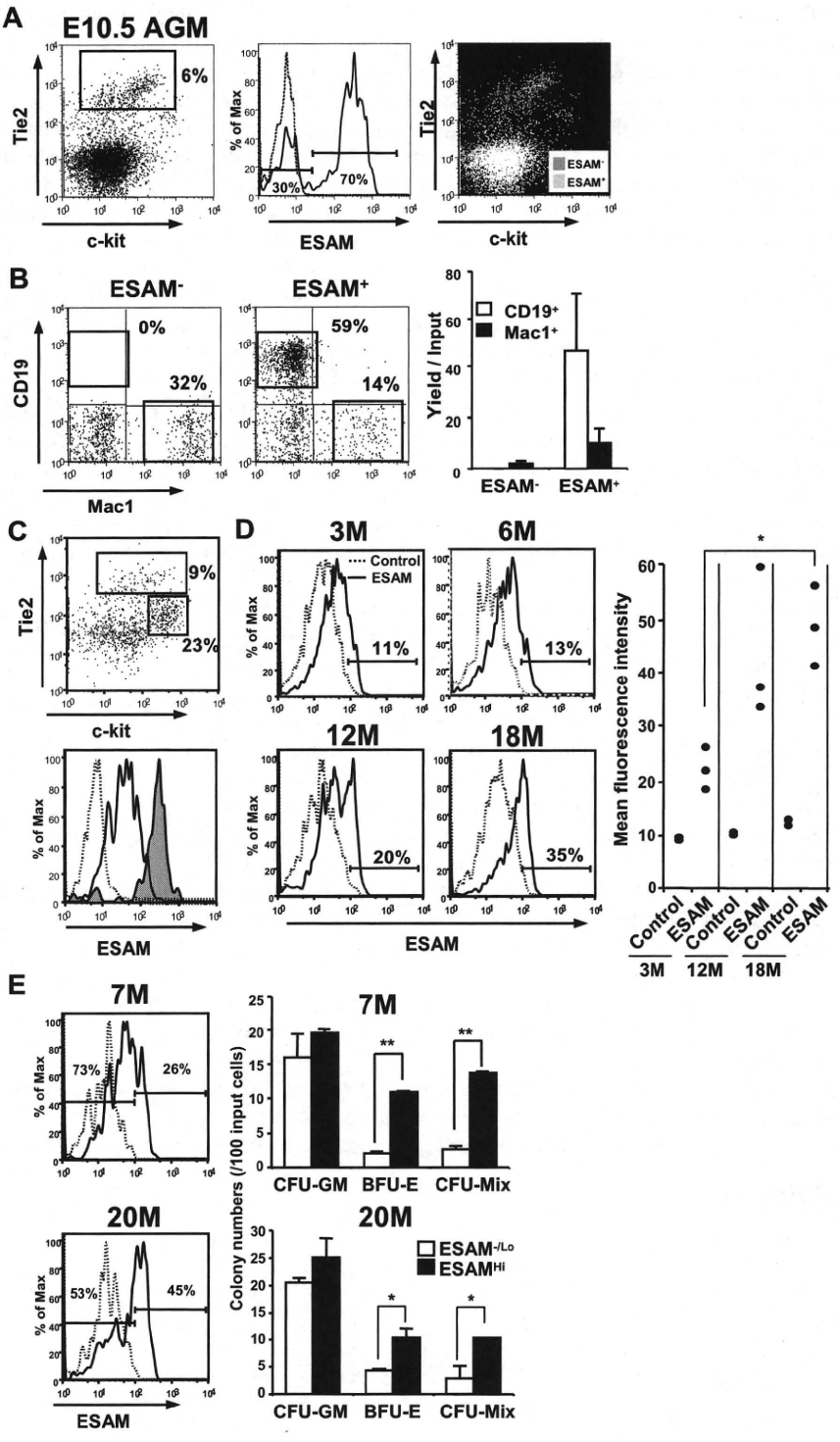

Figure 7. ESAM marks early hematopoietic progenitors throughout life. (A) Rag1/GFP$^-$ cells were sorted from AGM of E10.5 Rag1/GFP knockin heterozygous fetuses with high purity. The sorted Rag1/GFP$^-$ cells were incubated with the anti-ESAM Ab (1G8) followed by goat antirat IgG-FITC. The cells were then stained with anti-c-kit-APC, anti-Tie2-PE, and 7-AAD. The profile of Tie2 and c-kit expression in AGM cells was shown in a left panel. ESAM expression (solid line) in the Tie2^{Hi} fraction of AGM and its control level with an isotype-matched IgG (dashed line) are presented (middle). The Tie2^{Hi} ESAM$^+$ cells (yellow) were c-kit$^+$, whereas the Tie2^{Hi} ESAM$^-$ cells (pink) were c-kit$^-$ (right). (B) The Tie2^{Hi} ESAM$^-$ and Tie2^{Hi} ESAM$^+$ cells were sorted from E10.5 AGM and cultured on MS5 for 10 days. The recovered cells were counted and stained for the markers, including CD19 and Mac1. (C) Rag1/GFP$^-$ cells sorted from E10.5 YS were stained in the same manner as for the E10.5 AGM cells described in panel A. The profile of Tie2 and c-kit expression is shown in the top panel. In the lower panel, ESAM expression in the Tie2^{Hi} c-kit^{Lo} fraction (tinted histogram) and the Tie2^{Lo} c-kit^{Hi} fraction (open histogram) is shown. A dashed line shows the background fluorescence with an isotype-matched IgG. (D) ESAM expression of Rag1/GFP$^-$ Lin$^-$ ckit^{Hi} Sca1$^+$ cells of adult bone marrow of 3-, 6-, 12-, and 18-month-old mice was analyzed. Representative flow cytometry results in 3 to 5 mice of each age were shown. ESAM expression on Rag1/GFP$^-$ Lin$^-$ c-kit^{Hi} Sca1$^+$ cells of adult bone marrow of 3-, 12-, and 18-month-old mice (n = 3 in each) were simultaneously analyzed, and the data were summarized with respect to the mean fluorescence intensity with an anti-ESAM Ab or its control Ab (right panel). (E) ESAM$^{-/Lo}$ or ESAM^{Hi} cells were sorted from the Rag1/GFP$^-$ Lin$^-$ ckit^{Hi} Sca1$^+$ fraction of the indicated adult bone marrow (7 and 20 months old, respectively) and subjected to methylcellulose colony assay. The data are from one of 2 independent experiments that gave similar results. Statistical significance: $^*P < .05$, $^{**}P < .01$. The percentages of cells in each gate are indicated in each panel.

knockin reporters and with fewer combinations of Abs to obtain highly enriched HSCs.

Although we identified *Esam* as one of the highly expressed genes in HSC but not in ELP, levels of this antigen strongly correlated with lymphopoietic activity. The ESAM^{Hi} fraction in Rag1$^-$ c-kit^{Hi} Sca1$^+$ cells of E14.5 fetal liver produced CD19$^+$ B-lineage cells more effectively and contained lymphopoietic progenitors with even higher frequency than the ESAM$^{-/Lo}$ fraction. The cells also gave rise to long-term reconstitution in both T and B lymphoid lineages in lethally irradiated recipients. Furthermore, in the PSp/AGM region, B lymphopoietic activity in culture was exclusive to the ESAM^{Hi} Tie2$^+$ fraction. From these observations, we conclude that ESAM expression indicates high lymphopoietic potential in HSCs of the fetal liver and hematopoietic cells arising in the AGM region. On the other hand, we presume from the sharp down-regulation in ELPs that ESAM is not necessary for early lymphoid differentiation.

We previously reported that the first lymphopoietic cells arise in a Tie2$^+$ c-kit$^+$ CD34$^{-/Lo}$ CD41$^-$ subset in the E8.5 PSp region.[19] In this report, we showed clear ESAM expression on lymphopoietic

cells contained in a Tie2^{Hi} c-kit^{+} subset of the E9.5 to E10.5 PSp/AGM. Lymphopoietic activity in early embryos is thought to associate closely with HSC development. Because the first HSCs have few reliable surface markers, high ESAM expression must be useful to monitor how the first HSCs are developing and moving to other sites. As an additional finding, we detected high myeloid-erythroid but little lymphopoietic potential in a Tie2^{Lo} ckit^{Hi} subset of the YS, whose expression level of ESAM was apparently low. We presume that ESAM^{Hi} Tie2^{Hi} c-kit^{+} cells in the PSp/AGM and ESAM^{Lo} Tie2^{Lo} c-kit^{Hi} cells in the YS differ in their origins and/or as development progresses. If combined with those cell surface markers, a newly described method to trace runt-related transcription factor 1-expressing cells would address several important issues related to "primitive" and "definitive" hematopoiesis.[33]

It is interesting to speculate that ESAM might be important for HSC functions. A previous study showed that ESAM mediates homophilic interactions between endothelial cells,[22] and endothelial cells must represent an important component of HSC-supportive niches in bone marrow.[34] A subsequent study of ESAM-deficient mice showed impaired migration of neutrophils through vascular walls after normal adhesion.[35] In addition, platelets from ESAM-deficient mice were less prone to disaggregation.[36] Thus, ESAM expressed by endothelial and/or stem cells could have functions associated with HSC adhesion and/or migration.

Osteoblastic stromal cells that line trabecular bone are thought to construct niches containing molecules needed to regulate HSC quiescence, proliferation, and differentiation in adult bone marrow.[37,38] Other findings indicate that HSCs also interact with sinusoidal endothelial cells at some distance from bones.[39,40] Osteoblastic and vascular niches probably function in complementary ways.[41,42] The fetal liver has no osteoblasts, and HSC niches have not been identified in that site. High level ESAM display suggests that it should be further explored within the context of endothelial-HSC interactions.

It was an unexpected but intriguing finding that ESAM levels correlate with the stem cell rich fraction even in 22-month-old mice. Although many endothelial antigens on HSCs decline with aging, endomucin and endothelial protein C receptor (CD201) have been reported to be adult HSC markers.[17,43] In humans, angiotensin-converting enzyme (CD143) was recently found to mark HSCs through embryonic and adult life.[44] However, ESAM seems unique in actually increasing with aging. Many genes involved in NO-mediated signal transduction, stress responses, and inflammation have been linked to HSC aging.[4] P-selectin is one of the most highly up-regulated of those stress-related genes. Of particular interest, P-selectin mediates some leukocyte-vascular endothelium interactions and leukocyte extravasation, functions also attributed to ESAM on neutrophils.[35] Recent reports showed that stem/progenitor cells continuously circulate outside bone marrow and can actively participate in innate immune responses.[45,46] Furthermore, platelets can use P-selectin to recruit marrow hematopoietic cells into sites of injury.[47] Although direct evidence is lacking at this moment, further study might implicate elevated ESAM levels in extramedullary migration of HSCs.

Efficient HSC-based therapies and the emerging field of regenerative medicine will benefit from learning more about what defines stem cells. Although patterns of expression of transcription factors and other intracellular proteins are informative, surface markers such as ESAM that are unique to HSCs have special utility.

Acknowledgment

The authors thank Drs N. Sakaguchi (Kumamoto University) and H. Igarashi (Kawasaki Medical School) for the Rag1/GFP knockin mice.

Authorship

Contribution: T.Y. conducted experiments and analyzed results; T.Y., K.O., P.W.K., and Y.K. designed the research plan and wrote the paper; S.B. and D.V. prepared anti-ESAM antibodies; K.K. and T.M. performed and analyzed microarrays.

Conflict-of-interest disclosure: The authors declare no competing financial interests.

Correspondence: Takafumi Yokota, Department of Hematology and Oncology, Osaka University Graduate School of Medicine, C9, 2-2 Yamadaoka, Suita, Osaka 565-0871, Japan; e-mail: yokotat@bldon.med.osaka-u.ac.jp.

References

1. Osawa M, Hanada K, Hamada H, Nakauchi H. Long-term lymphohematopoietic reconstitution by a single CD34-low/negative hematopoietic stem cell. Science. 1996;273:242-245.
2. Spangrude GJ, Brooks DM. Mouse strain variability in the expression of the hematopoietic stem cell antigen Ly-6A/E by bone marrow cells. Blood. 1993;82:3327-3332.
3. Ogawa M. Changing phenotypes of hematopoietic stem cells. Exp Hematol. 2002;30:3-6.
4. Chambers SM, Shaw CA, Gatza C, Fisk CJ, Donehower LA, Goodell MA. Aging hematopoietic stem cells decline in function and exhibit epigenetic dysregulation. PLoS Biol. 2007;5:e201.
5. Yilmaz OH, Kiel MJ, Morrison SJ. SLAM family markers are conserved among hematopoietic stem cells from old and reconstituted mice and markedly increase their purity. Blood. 2006;107:924-930.
6. Takahashi K, Tanabe K, Ohnuki M, et al. Induction of pluripotent stem cells from adult human fibroblasts by defined factors. Cell. 2007;131:861-872.
7. Hanna J, Wernig M, Markoulaki S, et al. Treatment of sickle cell anemia mouse model with iPS cells generated from autologous skin. Science. 2007;318:1920-1923.
8. Nishikawa SI, Nishikawa S, Kawamoto H, et al. In vitro generation of lymphohematopoietic cells from endothelial cells purified from murine embryos. Immunity. 1998;8:761-769.
9. Oberlin E, Tavian M, Blazsek I, Péault B. Blood-forming potential of vascular endothelium in the human embryo. Development. 2002;129:4147-4157.
10. Yoder MC, Hiatt K, Dutt P, Mukherjee P, Bodine DM, Orlic D. Characterization of definitive lymphohematopoietic stem cells in the day 9 murine yolk sac. Immunity. 1997;7:335-344.
11. Takakura N, Huang XL, Naruse T, et al. Critical role of the TIE2 endothelial cell receptor in the development of definitive hematopoiesis. Immunity. 1998;9:677-686.
12. Cho SK, Bourdeau A, Letarte M, Zúñiga-Pflücker JC. Expression and function of CD105 during the onset of hematopoiesis from Flk1(+) precursors. Blood. 2001;98:3635-3642.
13. Matsuoka S, Ebihara Y, Xu M, et al. CD34 expression on long-term repopulating hematopoietic stem cells changes during developmental stages. Blood. 2001;97:419-425.
14. Sato T, Laver JH, Ogawa M. Reversible expression of CD34 by murine hematopoietic stem cells. Blood. 1999;94:2548-2554.
15. Tajima F, Sato T, Laver JH, Ogawa M. CD34 expression by murine hematopoietic stem cells mobilized by granulocyte colony-stimulating factor. Blood. 2000;96:1989-1993.
16. Randall TD, Weissman IL. Phenotypic and functional changes induced at the clonal level in hematopoietic stem cells after 5-fluorouracil treatment. Blood. 1997;89:3596-3606.
17. Matsubara A, Iwama A, Yamazaki S, et al. Endomucin, a CD34-like sialomucin, marks hematopoietic stem cells throughout development. J Exp Med. 2005;202:1483-1492.
18. Yokota T, Kouro T, Hirose J, et al. Unique properties of fetal lymphoid progenitors identified according to RAG1 gene expression. Immunity. 2003;19:365-375.
19. Yokota T, Huang J, Tavian M, et al. Tracing the first waves of lymphopoiesis in mice. Development. 2006;133:2041-2051.

20. Kuwata N, Igarashi H, Ohmura T, Aizawa S, Sakaguchi N. Cutting edge: absence of expression of RAG1 in peritoneal B-1 cells detected by knocking into RAG1 locus with green fluorescent protein gene. J Immunol. 2001;163:6355-6359.
21. Igarashi H, Gregory SC, Yokota T, Sakaguchi N, Kincade PW. Transcription from the RAG1 locus marks the earliest lymphocyte progenitors in bone marrow. Immunity. 2002;17:117-130.
22. Nasdala I, Wolburg-Buchholz K, Wolburg H, et al. A transmembrane tight junction protein selectively expressed on endothelial cells and platelets. J Biol Chem. 2002;277:16294-16303.
23. Yuasa H, Oike Y, Iwama A, et al. Oncogenic transcription factor Evi1 regulates hematopoietic stem cell proliferation through GATA-2 expression. EMBO J. 2005;24:1976-1987.
24. Mikkola HK, Fujiwara Y, Schlaeger TM, Traver D, Orkin SH. Expression of CD41 marks the initiation of definitive hematopoiesis in the mouse embryo. Blood. 2003;101:508-516.
25. Akashi K, Traver D, Miyamoto T, Weissman IL. A clonogenic common myeloid progenitor that gives rise to all myeloid lineages. Nature. 2000;404:193-197.
26. Kim I, He S, Yilmaz OH, Kiel MJ, Morrison SJ. Enhanced purification of fetal liver hematopoietic stem cells using SLAM family receptors. Blood. 2006;108:737-744.
27. Cumano A, Dieterlen-Lievre F, Godin I. Lymphoid potential, probed before circulation in mouse, is restricted to caudal intraembryonic splanchnopleura. Cell. 1996;86:907-916.
28. Medvinsky A, Dzierzak E. Definitive hematopoiesis is autonomously initiated by the AGM region. Cell. 1996;86:897-906.
29. de Bruijn MF, Ma X, Robin C, Ottersbach K, Sanchez MJ, Dzierzak E. Hematopoietic stem cells localize to the endothelial cell layer in the midgestation mouse aorta. Immunity. 2002;16:673-683.
30. Forsberg EC, Prohaska SS, Katzman S, Heffner GC, Stuart JM, Weissman IL. Differential expression of novel potential regulators in hematopoietic stem cells. PLoS Genet. 2005;1:e28.
31. Hirata Ki, Ishida T, Penta K, et al. Cloning of an immunoglobulin family adhesion molecule selectively expressed by endothelial cells. J Biol Chem. 2001;276:16223-16231.
32. Kincade PW, Owen JJ, Igarashi H, Kouro T, Yokota T, Rossi MI. Nature or nurture? Steady-state lymphocyte formation in adults does not recapitulate ontogeny. Immunol Rev. 2002;187:116-125.
33. Samokhvalov IM, Samokhvalova NI, Nishikawa SI. Cell tracing shows the contribution of the yolk sac to adult haematopoiesis. Nature. 2007;446:1056-1061.
34. Yao L, Yokota T, Xia L, Kincade PW, McEver RP. Bone marrow dysfunction in mice lacking the cytokine receptor gp130 in endothelial cells. Blood. 2005;106:4093-4101.
35. Wegmann F, Petri B, Khandoga AG, et al. ESAM supports neutrophil extravasation, activation of Rho, and VEGF-induced vascular permeability. J Exp Med. 2006;203:1671-1677.
36. Brass LF, Zhu L, Stalker TJ. Novel therapeutic targets at the platelet vascular interface. Arterioscler Thromb Vasc Biol. 2008;28[suppl]:S43-S50.
37. Zhang J, Niu C, Ye L, et al. Identification of the haematopoietic stem cell niche and control of the niche size. Nature. 2003;425:836-841.
38. Calvi LM, Adams GB, Weibrecht KW, et al. Osteoblastic cells regulate the haematopoietic stem cell niche. Nature. 2003;425:841-846.
39. Kiel MJ, Yilmaz OH, Iwashita T, Yilmaz OH, Terhorst C, Morrison SJ. SLAM family receptors distinguish hematopoietic stem and progenitor cells and reveal endothelial niches for stem cells. Cell. 2005;121:1109-1121.
40. Sugiyama T, Kohara H, Noda M, Nagasawa T. Maintenance of the hematopoietic stem cell pool by CXCL12-CXCR4 chemokine signaling in bone marrow stromal cell niches. Immunity. 2006;25:977-988.
41. Yin T, Li L. The stem cell niches in bone. J Clin Invest. 2006;116:1195-1201.
42. Orford KW, Scadden DT. Deconstructing stem cell self-renewal: genetic insights into cell-cycle regulation. Nat Rev Genet. 2008;9:115-128.
43. Balazs AB, Fabian AJ, Esmon CT, Mulligan RC. Endothelial protein C receptor (CD201) explicitly identifies hematopoietic stem cells in murine bone marrow. Blood. 2006;107:2317-2321.
44. Jokubaitis VJ, Sinka L, Driessen R, et al. Angiotensin-converting enzyme (CD143) marks hematopoietic stem cells in human embryonic, fetal, and adult hematopoietic tissues. Blood. 2008;111:4055-4063.
45. Massberg S, Schaerli P, Knezevic-Maramica I, et al. Immunosurveillance by hematopoietic progenitor cells trafficking through blood, lymph, and peripheral tissues. Cell. 2007;131:994-1008.
46. Welner RS, Kincade PW. Stem cells on patrol. Cell. 2007;131:842-844.
47. Massberg S, Konrad I, Schürzinger K, et al. Platelets secrete stromal cell-derived factor 1alpha and recruit bone marrow-derived progenitor cells to arterial thrombi in vivo. J Exp Med. 2006;203:1221-1233.

THE JOURNAL OF BIOLOGICAL CHEMISTRY VOL. 285, NO. 41, pp. 31774–31782, October 8, 2010

BCR-ABL but Not JAK2 V617F Inhibits Erythropoiesis through the Ras Signal by Inducing p21$^{CIP1/WAF1}$*[S]

Received for publication, February 28, 2010, and in revised form, July 24, 2010 Published, JBC Papers in Press, July 27, 2010, DOI 10.1074/jbc.M110.118653

Masahiro Tokunaga[‡], Sachiko Ezoe[‡§1], Hirokazu Tanaka[‡], Yusuke Satoh[‡], Kentaro Fukushima[‡], Keiko Matsui[‡], Masaru Shibata[‡], Akira Tanimura[‡], Kenji Oritani[‡], Itaru Matsumura[‡¶], and Yuzuru Kanakura[‡]

From the [‡]Department of Hematology and Oncology, Osaka University Graduate School of Medicine, 2-2 Yamada-oka, Suita, Osaka 565-0871, the [§]Medical Center of Translational Research, Osaka University Hospital, Suita, Osaka 565-0871, and the [¶]Division of Hematology, Department of Internal Medicine, Kinki University School of Medicine, Osaka-Sayama, Osaka 589-8511, Japan

BCR-ABL is a causative tyrosine kinase (TK) of chronic myelogenous leukemia (CML). In CML patients, although myeloid cells are remarkably proliferating, erythroid cells are rather decreased and anemia is commonly observed. This phenotype is quite different from that observed in polycythemia vera (PV) caused by JAK2 V617F, whereas both oncogenic TKs activate common downstream molecules at the level of hematopoietic stem cells (HSCs). To clarify this mechanism, we investigated the effects of BCR-ABL and JAK2 V617F on erythropoiesis. Enforced expression of BCR-ABL but not of JAK2 V617F in murine LSK (Lineage$^-$Sca-1^{hi}CD117^{hi}) cells inhibited the development of erythroid cells. Among several signaling molecules downstream of BCR-ABL, an active mutant of N-Ras (N-RasE12) but not of STAT5 or phosphatidylinositol 3-kinase (PI3-K) inhibited erythropoiesis, while N-RasE12 enhanced the development of myeloid cells. BCR-ABL activated Ras signal more intensely than JAK2 V617F, and inhibition of Ras by manumycin A, a farnesyltransferase inhibitor, ameliorated erythroid colony formation of CML cells. As for the mechanisms of Ras-induced suppression of erythropoiesis, we found that GATA-1, an erythroid-specific transcription factor, blocked Ras-mediated mitogenic signaling at the level of MEK through the direct interaction. Furthermore, enforced expression of N-RasE12 in LSK cells derived from p53-, p16^{INK4a}/p19^{ARF}-, and p21$^{CIP1/WAF1}$-null/wild-type mice revealed that suppressed erythroid cell growth by N-RasE12 was restored only by p21$^{CIP1/WAF1}$ deficiency, indicating that a cyclin-dependent kinase (CDK) inhibitor, p21$^{CIP1/WAF1}$, plays crucial roles in Ras-induced suppression of erythropoiesis. These data would, at least partly, explain why respective oncogenic TKs cause different disease phenotypes.

Oncogenic tyrosine kinases (TKs)[2] such as BCR-ABL, FLT3-ITD, and JAK2 V617F are known to confer growth and/or survival advantage on hematopoietic cells, thereby causing hematologic malignancies (1–3). These gene alterations are supposed to occur at the hematopoietic stem cell (HSC) level (3, 4). Although these oncogenic TKs activate common downstream pathways including Ras/Raf/MEK/ERK, PI3-K/Akt, and STAT (1, 2, 5), their disease phenotypes are quite different: BCR-ABL is a causative gene of chronic myelogenous leukemia (CML) (1), FLT3-ITD of acute myeloid leukemia (AML) (2), and JAK2 V617F of myeloproliferative neoplasms including polycythemia vera (PV), essential thrombocythemia (ET) and primary myelofibrosis (PMF) (3). In patients with chronic-phase CML, anemia is a common feature in contrast to the marked leukocytosis in the peripheral blood. Also, bone marrow (BM) examination shows that erythroid islands are reduced in number and size despite the increased cellularity due to the granulocytic proliferation (6). This disease phenotype is totally different from that of PV, in which JAK2 V617F causes erythrocytosis together with the mild leukocytosis and thrombocytosis. Furthermore, in blast-phase CML, blast lineages are generally myeloid or lymphoid, and erythroid crisis is a rare incidence with a frequency no more than 5% (7, 8). These data suggest that, in contrast to the trilinear promoting activities of JAK2 V617F, BCR-ABL might not support the development of erythroid cells.

BCR-ABL activates several downstream pathways including Ras/Raf/MEK/ERK, STAT5, and PI3-K/Akt pathways (1, 4). Among them, we have previously shown that Ras plays crucial roles in the growth and survival of BCR-ABL-positive K562 cells, while STAT5 and PI3-K pathways contribute to their growth and survival to the only limited extent (9). In addition, although the role of STAT5 in BCR-ABL-mediated leukemogenesis remains controversial (10, 11), another group also reported that transformation of murine BM cells by BCR-ABL is blocked by dominant-negative Ras (12). Furthermore, Ras signaling was shown to be indispensable for the pathogenesis of CML in a murine BM transplantation model (13). Therefore, the activated Ras is considered to be essential for the pathogenesis of CML, and is also speculated to principally determine the disease phenotype of CML, that is, prominent proliferation of myeloid cells accompanied by the suppressed erythropoiesis.

* This work was supported by grants from the Ministry of Education, Science, Sports, and Culture and Technology of Japan.

[S] The on-line version of this article (available at http://www.jbc.org) contains supplemental Table S1 and Methods.

[1] To whom correspondence should be addressed. Tel.: 81-6-6879-3871; Fax: 81-6-6879-3879; E-mail: sezoe@bldon.med.osaka-u.ac.jp.

[2] The abbreviations used are: TK, tyrosine kinase; CML, chronic myelogenous leukemia; PV, polycythemia vera; HSC, hematopoietic stem cell; LSK, Lineage$^-$Sca-1^{hi}CD117^{hi}; BM, bone marrow; CDK, cyclin-dependent kinase; rh, recombinant human; TPO, thrombopoietin; rm, recombinant murine; EPO, erythropoietin; SCF, stem cell factor; G1ERT, GATA-1/ERT; 4-HT, 4-hydroxytamoxifen; Ab, antibody; HPRT, hypoxanthine phosphoribosyl transferase; pRb, retinoblastoma protein; PRAK, p38-regulated/activated protein kinase.

Ras is constitutively activated by various oncogenic TKs or mutations of Ras itself in various malignant tumors. Although oncogenic (or constitutively activated) Ras was originally shown to transmit mitogenic and survival signals through Raf/MEK/ERK (14), recent studies have demonstrated that, like other oncogenic stimuli, it also induces growth inhibition/arrest in normal cells to prevent their malignant transformation. In general, this biological phenomenon is called "cellular senescence" and observed in various types of non-hematopoietic cells (15, 16). In addition, excessive Ras signaling was reported to inhibit erythropoiesis (17, 18), indicating the presence of a similar cellular response in hematopoietic cells. So far, oncogenic Ras has been shown to cause senescence through several signaling pathways other than Raf/MEK/ERK (15, 19–21). Also, several cell cycle regulatory molecules such as p53, p16^{INK4a}, p19^{ARF} and p21$^{CIP1/WAF1}$, have been shown to play central roles in oncogene-induced senescence (15, 19, 21).

In this report, we found that BCR-ABL but not JAK2 V617F, and among their downstream molecules, Ras but not STAT5 or PI3-K suppress erythropoiesis from murine LSK cells. As for this mechanism, we found that an erythroid-lineage specific transcription factor, GATA-1, blocks Ras-dependent growth and survival by inhibiting MEK1 activity through the direct interaction. Furthermore, we showed that a cyclin-dependent kinase (CDK) inhibitor, p21$^{CIP1/WAF1}$, plays crucial roles in Ras-induced suppression of erythropoiesis using p21$^{CIP1/WAF1}$-deficient hematopoietic cells.

EXPERIMENTAL PROCEDURES

Cytokines and Reagents—Recombinant human thrombopoietin (rhTPO) and recombinant murine interleukin-3 (rmIL-3) were provided by Kyowa Hakko Kirin (Tokyo, Japan). Recombinant human erythropoietin (rhEPO) and murine stem cell factor (rmSCF) were purchased from R & D Systems (Minneapolis, MN). Manumycin A was purchased from Merck KGaA (Darmstadt, Germany).

Plasmid Constructs and cDNAs—Expression vectors for GATA-1/ERT (G1ERT) and wild-type (WT) GATA-1 were described previously (22). Active forms of N-Ras (N-RasE12) (23) and STAT5A (1*6 STAT5A) (24), and membrane-targeted PI3-K catalytic subunit (p110^{CAAX}) (25) were subcloned into pMYs-IRES-EGFP, a retrovirus expression vector, which was kindly provided by Dr. T. Kitamura (University of Tokyo, Tokyo, Japan). pMSCV-IRES-GFP-p210-BCR-ABL is a generous gift from Dr. C. J. Eaves (Terry Fox Laboratory, Vancouver, BC, Canada) (26). The cDNA of JAK2 V617F was kindly provided by Dr. K. Shimoda (University of Miyazaki, Miyazaki, Japan) (27) and was subcloned into pMSCV-IRES-GFP.

Cell Lines and Cultures—A murine IL-3-dependent hematopoietic cell line, Ba/F3, was maintained in RPMI (nacalai tesque, Kyoto, Japan) supplemented with 10% fetal bovine serum (FBS) (Equitech-Bio, Kerrville, TX) and 0.3 ng/ml rmIL-3. NIH3T3 and 293T cells were cultured in Dulbecco's modified Eagle's medium (DMEM; nacalai tesque) supplemented with 10% FBS.

Preparation of Stable Transformants from Ba/F3—We introduced G1ERT into Ba/F3 cells by electroporation (250 V and 950 microfarads) and selected stably transfected clones by the culture with G-418 (1.0 mg/ml; Wako Pure Chemical Industries, Osaka, Japan). We further introduced pMYs-IRES-EGFP-N-RasE12 and obtained doubly transfected clones by sorting GFP-positive cells with BD FACSAria Cell-Sorting System (BD Biosciences, San Jose, CA). Their IL-3-independent growth and cell cycle were analyzed with or without the activation of GATA-1 by 4-hydroxytamoxifen (4-HT; Sigma-Aldrich). DNA contents of the cells were evaluated by staining with propidium iodide.

Luciferase Assays—Luciferase assays were performed with a Dual-Luciferase Reporter Assay System (Promega, Madison, WI) as previously described (22). As for assays using Ba/F3 cells, transfection was performed with Amaxa Nucleofector technology (Lonza, Cologne, Germany), followed by the measurement of luciferase activities after 24 h.

Immunoblotting and Coimmunoprecipitation Analyses—Preparation of cell lysates, immunoprecipitation, gel electrophoresis, and immunoblotting were performed according to the methods described previously (22, 28). Antibodies (Abs) and reagents were supplied by the manufacturers described in supplemental methods.

Glutathione S-transferase (GST) Pull-down Assays—GST pull-down assays were performed as previously reported (22).

Animals—The congenic C57BL/6J mice were purchased from Clea Japan, Inc. (Tokyo, Japan). B6.129-Cdkn2a^{tm1Rdp} (p16^{INK4a}/p19^{ARF}-null) mice and p53-null mice were kindly provided by Technology Transfer Center National Cancer Institute (Rockville, MD) and Dr. N. Nishimoto (Wakayama Medical University, Wakayama, Japan), respectively. B6.129S2-Cdkn1a^{tm1Tyj}/J (p21$^{CIP1/WAF1}$-null) mice were purchased from The Jackson Laboratory (Bar Harbor, ME). The experimental designs of this study were approved by the Institutional Animal Care and Use Committee at Osaka University Graduate School of Medicine.

Separation of Murine Hematopoietic Progenitors—Murine BM cells were flushed from both femora and tibiae, and progenitors were concentrated by anti-mouse CD117 MicroBeads and autoMACS Pro Separator (Miltenyi Biotec, Bergisch Gladbach, Germany). To isolate LSK (Lineage$^-$Sca-1^{hi}CD117^{hi}) cells, selected progenitors were stained with phycoerythrin-conjugated (PE-conjugated) monoclonal Abs against murine lineage markers (CD3e (145–2C11), CD45R/B220 (RA3–6B2), Gr-1 (RB6–8C5), CD11b (M1/70), and TER-119 (TER-119)), fluorescein isothiocyanate-conjugated (FITC-conjugated) anti-Sca-1 Ab (E13–161.7), and allophycocyanin-conjugated (APC-conjugated) anti-CD117 Ab (2B8), and isolated by FACSAria. All Abs were purchased from BD Biosciences.

Preparation of Retrovirus Particles—Preparation of retrovirus particles was performed as described previously (29) (see supplemental methods).

Retrovirus Transfection into Murine BM Progenitors—Isolated LSK cells were precultured overnight in DMEM supplemented with 10% FBS, rmSCF (100 ng/ml), and rhTPO (100 ng/ml). Then, the cells were seeded on 24-well tissue plates coated with RetroNectin (TaKaRa Bio Inc., Shiga, Japan), infected with each viral supernatant by spinoculation, and cultured in the same medium containing 10% FBS, protamine sulfate (10 μg/ml; Sigma-Aldrich), rmSCF (50 ng/ml), and rhTPO (50 ng/ml). After 48 h of culture, retrovirus-transduced GFP$^+$

cells were sorted with FACSAria and were subjected to colony assays or stromal coculture.

Colony Assays—Cells were plated at the indicated density in methylcellulose medium (MethoCult; Stem Cell Technologies, Vancouver, BC, Canada) supplemented with the indicated growth factors. Cells were incubated with 5% CO_2 at 37 °C, and the numbers of colonies were counted after the indicated days.

Stromal Coculture—A murine BM stromal cell line, MS-5, was cultured in minimum essential medium (MEM) α (Invitrogen, Carlsbad, CA) with 10% FBS and prepared in 24-well tissue plates 1 day before the seeding. The sorted GFP$^+$ progenitors were seeded (1.5×10^3 cells/well) on the monolayer of MS-5 and cocultured in 2 ml of MEMα supplemented with 10% FBS, rmSCF (50 ng/ml), and rhEPO (3 units/ml). Five days after the initiation of coculture, hematopoietic cells were harvested and stained with PE-conjugated anti-CD45 (30-F11) Ab, and APC-conjugated anti-CD11b (M1/70) or anti-TER-119 (TER-119) Ab (all of them from BD Biosciences). To evaluate the phosphorylation status of ERK1/2, we used BD Phosflow technology (BD Biosciences). The harvested cells were further incubated in DMEM containing 2% FBS without cytokines for 4 h, then fixed, permeabilized, and stained with Alexa Fluor®647-conjugated anti-ERK1/2 (pT202/pY204) Ab (BD Biosciences) according to the manufacturer's recommendation.

Flow Cytometric Analyses—Flow cytometric analyses were performed using BD FACSCanto II (BD Biosciences). The data analyses were done with BD FACSDiva software (BD Biosciences) or FlowJo software (TreeStar, Ashland, OR).

Immunofluorescence Microscopy—5×10^4 of the transduced cells were cytospun onto microscope slides, fixed in 2% paraformaldehyde, and permeabilized in 1% Nonidet P-40 in PBS. After the incubation in blocking buffer (1 mg/ml of γ-globulin in PBS), the slides were incubated with a monoclonal Ab against p16^{INK4a} (F-12) or p19^{ARF} (5-C3–1) (both from Santa Cruz Biotechnology, Santa Cruz, CA). The slides were then incubated with an Alexa Fluor®546-conjugated secondary antibody (goat anti-mouse IgG for p16^{INK4a}, or goat anti-rat IgG for p19^{ARF}), followed by the staining of nuclei with Hoechst 33342 (all from Invitrogen). The slides were mounted in Fluoromount (Diagnostic BioSystems, Pleasanton, CA) before viewing on a LSM 5 PASCAL microscope (Carl Zeiss, Oberkochen, Germany).

Semiquantitative RT-PCR—Total RNA was isolated from 5×10^3 of the transduced cells using RNeasy Mini Kit (Qiagen, Hilden, Germany) and converted to cDNA by SuperScript III First Strand Synthesis System (Invitrogen). PCR was performed using Ampli Taq Gold (Applied Biosystems, Carlsbad, CA) with primers described in supplemental Table S1.

Real-time RT-PCR—Quantitative real-time RT-PCR was performed using FastStart Universal SYBR Green Master (Roche Diagnostics GmbH, Mannheim, Germany) and PRISM 7900HT (Applied Biosystems). Amplified signals were normalized to the levels of hypoxanthine phosphoribosyl transferase (HPRT). The primer sequences are described in supplemental Table S1.

BM Samples from CML Patients—BM samples were obtained from three patients with newly diagnosed chronic-phase CML. CD34$^+$ cells were separated using the MACS immunomagnetic separation system, and were subjected to colony assays. All BM samples were obtained after receiving written informed consent in accordance with the Declaration of Helsinki, and this study protocol was approved by the institutional review board of Osaka University Hospital.

Statistical Methods—Statistical analyses were carried out by standard Student *t* tests. Error bars used throughout indicate S.D.

RESULTS

BCR-ABL but Not JAK2 V617F Inhibits the Development of Erythroid Cells—To examine the effects of BCR-ABL on erythropoiesis, we first introduced p210-BCR-ABL into murine LSK cells using the retrovirus vector harboring GFP as a reporter gene. After 48 h, GFP$^+$ cells were sorted and cocultured with a murine BM stromal cell line, MS-5, in the presence of rmSCF and rhEPO for 5 days. As compared with mock-transduced cells, the proportion of CD45^{low}TER-119$^+$ erythroid cells was reduced in BCR-ABL-transduced cells significantly (Fig. 1*A*). We also examined the effects of JAK2 V617F on erythropoiesis with the same strategy and found that JAK2 V617F did not reduce the proportion of erythoroid cells. In colony assays, BCR-ABL significantly decreased the number of burst-forming units-erythroid (BFU-E), while it increased the number of myeloid colonies (Fig. 1*B*). On the other hand, JAK2 V617F did not reduce the number of BFU-E. These data indicate that BCR-ABL but not JAK2 V617F inhibits the development of erythroid cells from murine hematopoietic progenitors.

Oncogenic Ras Inhibits Erythropoiesis Downstream of BCR-ABL—BCR-ABL activates mainly Ras/Raf/MEK/ERK, JAK2/STAT5, and PI3-K/Akt pathways. Next, to examine the roles of these pathways in erythropoiesis, we transduced LSK cells with an active form of each signal transduction molecule: N-RasE12 for an active form of N-Ras, 1*6 STAT5A for STAT5, and p110^{CAAX} for PI3-K. Compared with Mock, 1*6 STAT5A and p110^{CAAX} increased total erythroid cell numbers by 2.8- and 1.9-fold, respectively (both, $p < 0.05$), while the proportion of erythroid cells was scarcely influenced by both molecules due to the increase in total cell numbers (Fig. 2, *A* and *B*). In contrast, N-RasE12 remarkably reduced not only the frequency (Fig. 2*A*) but also the number of erythroid cells (0.28-fold) (Fig. 2*B*), while it significantly increased the number of CD11b$^+$-myeloid cells (Fig. 2*C*). We also performed colony assays using N-RasE12- or Mock-transduced LSK cells. As shown in Fig. 2*D*, N-RasE12 significantly reduced the number of BFU-E (average colony numbers from 1.0×10^3 cells input: Mock-transduced cells, 9.7; N-Ras-transduced cells, 0.33) ($p < 0.01$).

BCR-ABL Activates Ras Signal More Intensely than JAK2 V617F—Next, we tried to clarify why JAK2 V617F did not suppress erythropoiesis, because it has been reported to activate Ras as well as BCR-ABL (5). For this purpose, we introduced JAK2 V617F and BCR-ABL into murine LSK cells, cocultured them with MS-5, and evaluated the Ras activity by expediently measuring the phosphorylation status of ERK1/2 after 4-h starvation of cytokines. As shown in Fig. 2*E*, ERK1/2 was more intensely phosphorylated (activated) in cells transduced with BCR-ABL than in those with JAK2 V617F. We also examined the phosphorylation status of ERK1/2 in CML patients' blood

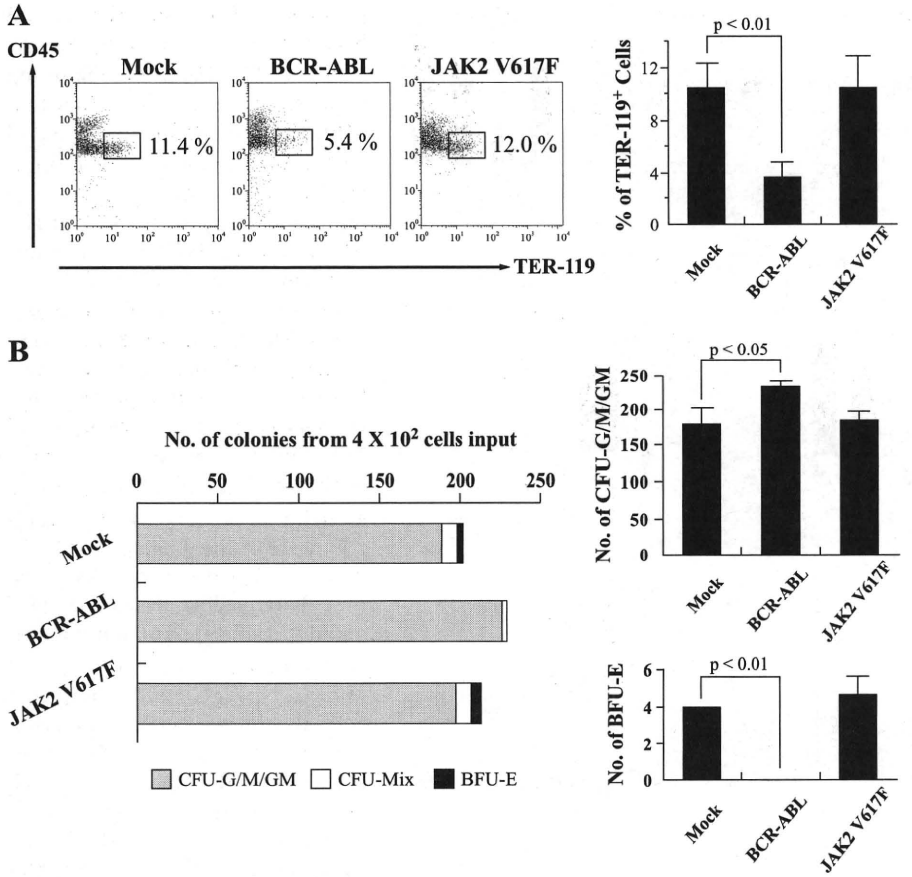

FIGURE 1. **Effects of oncogenic TKs on proliferation of erythroid cells.** *A*, after infection of retrovirus expressing Mock, BCR-ABL, or JAK2 V617F into murine LSK cells, GFP$^+$ cells were sorted and cocultured with MS-5 in the presence of rmSCF and rhEPO. After 5-day cultures, expression of CD45 and TER-119 was analyzed by flow cytometry (*left panels*). The proportions of CD45^{low}TER-119$^+$ cells are shown in the *right bar graph* ($n = 3$). *B*, respective retrovirus-transduced LSK cells were seeded at a density of 2.0×10^2 cells/35-mm dish in methylcellulose medium containing rmSCF, rmIL-3, rmIL-6, rhTPO, and rhEPO. Colony numbers were counted after 9 days. Representative colony numbers (*left*) and myeloid/erythroid colony numbers (*right*, $n = 3$) are shown. BFU-E, burst-forming units-erythroid; CFU-G/M/GM, colony-forming unit-granulocyte/macrophage/granulocyte-macrophage.

cells treated with manumycin A, a potent farnesyltransferase inhibitor which selectively suppresses Ras, or vehicle only. As shown in Fig. 2*F*, phosphorylation of ERK was reduced by Ras inhibition, indicating that BCR-ABL activates ERK through the activation of Ras. These data indicate that different growth status of erythroid cells between these TKs might result from the preferential activation of Ras signal by BCR-ABL.

Suppression of Ras Signal Ameliorates the Inhibition of Erythropoiesis Caused by BCR-ABL—Furthermore, to make sure that suppressed erythropoiesis caused by BCR-ABL is due to the activation of Ras signal, we examined the effects of Ras-inhibition on erythroid colony formation of BCR-ABL expressing cells. CD34$^+$ cells were separated from BM samples of three patients with newly diagnosed chronic-phase CML. They were then cultured in methylcellulose medium containing rhSCF, rhIL-3, and rhEPO, with or without manumycin A. Complete blockage of Ras signal by supplement of sufficient dose (10 μM) of manumycin A eradicated erythroid colony formation (data not shown). However, as shown in Fig. 2*G*, the number of erythroid colonies was restored by low doses of manumycin A in all three patients, though there was some difference in degree. This result, actually in primary CML cells, supports our model that, although Ras is indispensable for erythroid cell survival, excessive Ras signal downstream of BCR-ABL rather inhibits erythroid cell proliferation.

GATA-1 Inhibits Ras-dependent Cell Proliferation and Survival—As described above, oncogenic Ras signaling promoted the proliferation of myeloid cells, but inhibited that of erythroid cells. To elucidate the mechanisms underlying the different responses to oncogenic Ras between the two lineages, we examined the effects of GATA-1, which is expressed in erythroid cells but not in myeloid cells, on Ras signal. For this purpose, we transduced N-RasE12 and G1ERT, a chimera gene consisting of full-length GATA-1 and the mutated ligand-binding domain of estrogen receptor, into Ba/F3 cells, which was named Ba/F3/N-RasE12/G1ERT. G1ERT reveals GATA-1 activity in response to 4-HT as previously reported (22). As shown in Fig. 3*A*, N-RasE12 enabled this clone to proliferate and survive independently of IL-3. However, when GATA-1 activity was induced by 4-HT treatment, N-RasE12-dependent cell growth was completely suppressed (Fig. 3*A*). In agreement with this result, the proportion of growing cells in S-G2/M phase was reduced by 4-HT treatment from 36% to 8% in DNA contents analysis (Fig. 3*B*). Furthermore, 4-HT treatment induced apoptosis in 78% of cells, which was detected as a subdiploid fraction. From these results, we speculated that GATA-1 might inhibit oncogenic Ras activities, which transmit proliferation and survival signals.

GATA-1 Suppresses MEK Activity—Ras signal is known to be transmitted to the nucleus through Raf, MEK, and ERK in this order. To identify which molecule was inhibited by GATA-1 in this pathway, we performed luciferase assays using a reporter gene for ERK (3 × AP-1-Luc) in NIH3T3 and Ba/F3 cells. As shown in Fig. 4, *A* and *B*, GATA-1 significantly reduced the N-Ras- and MEK1-induced AP-1-luciferase activities almost to the baseline levels (*white boxes*), which indicates that GATA-1 inhibits Ras signal at the level or downstream of MEK. Next, we examined the phosphorylation status of MEK1/2 and ERK1/2 in Ba/F3/N-RasE12/G1ERT cells by immunoblot analysis. As shown in Fig. 4*C*, both MEK1/2 and ERK1/2 were phosphorylated by N-RasE12 even under the culture without IL-3, which was suppressed by 4-HT in a time-dependent manner. This

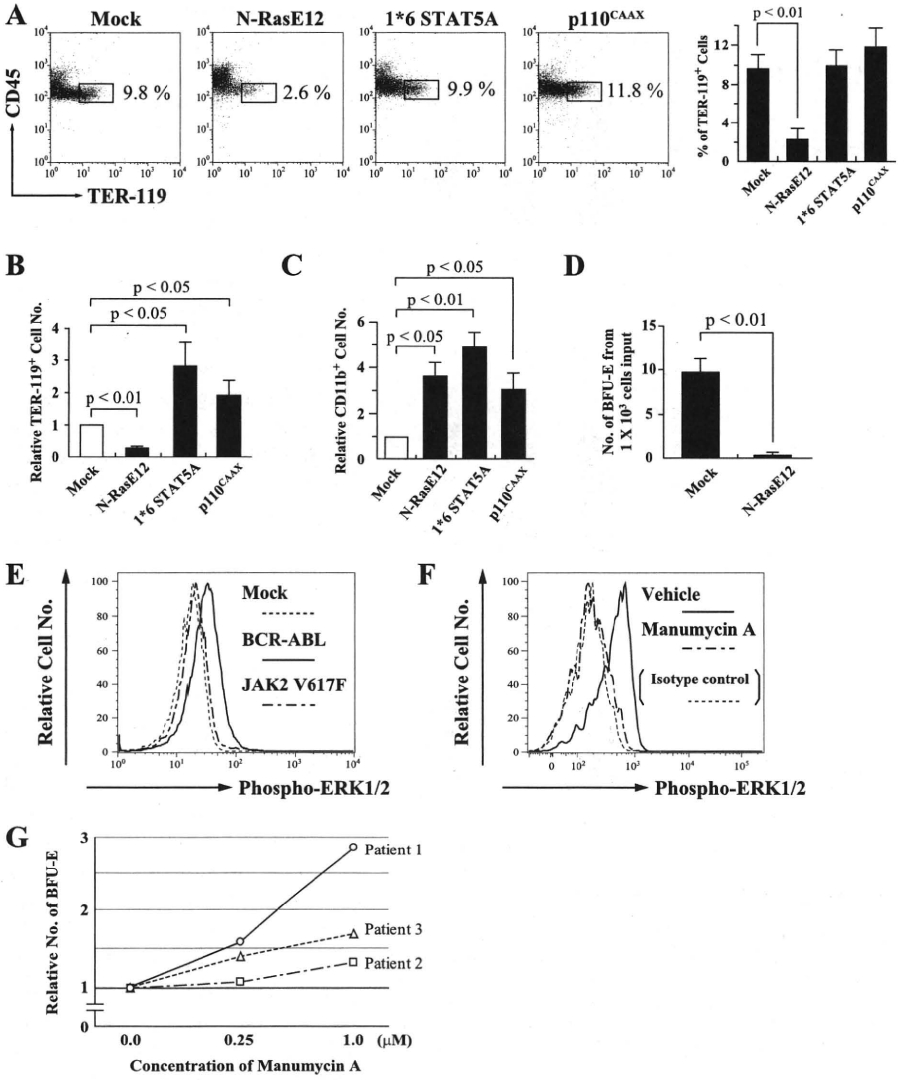

FIGURE 2. **Roles of downstream molecules of oncogenic TKs in erythropoiesis.** *A–C*, LSK cells each transfected with the indicated gene were cocultured with MS-5 in the medium containing rmSCF and rhEPO. After 5 days, expression of CD45 and TER-119 was analyzed by flow cytometry (*A*, *left panels*) and the proportions of CD45^{low}TER-119^{+} cells are shown (*A*, *right bar graph*, $n = 3$). Numbers of the TER-119^{+} cells were calculated by multiplication of the frequencies and total cell numbers. Relative numbers to Mock are shown (*B*). Relative CD11b^{+} myeloid cell numbers are shown (*C*). *D*, retrovirus-infected LSK cells were seeded at a density of 5.0×10^2 cells/dish in methylcellulose medium containing rmSCF, rmIL-3, and rhEPO. The numbers of BFU-E were counted after 8 days ($n = 3$). *E*, LSK cells, each transfected with Mock, BCR-ABL, or JAK2 V617F, were further incubated without cytokines after the coculture with MS-5, and the phosphorylation status of ERK1/2 was analyzed using Phosflow technology. *F*, after 5-h incubation of CML patients blood mononuclear cells with manumycin A (7 μM) or vehicle, the phosphorylation status of ERK1/2 was analyzed. *G*, CD34^{+} cells were separated from BM samples of three CML patients, and seeded in methylcellulose medium containing rhSCF, rhIL-3, and rhEPO, with manumycin A at the indicated concentrations or vehicle. The numbers of BFU-E were counted after 9 days, and shown as relative numbers to vehicle in each patient.

result implies that GATA-1 suppresses Ras signal at the level or upstream of MEK. Together with the results from luciferase assays, it was speculated that GATA-1 would inhibit MEK activity.

GATA-1 Blocks the Ras Signal through Its Direct Interaction with MEK1—To clarify how GATA-1 inhibits MEK activities, we examined the interaction between GATA-1 and MEK1. First, we transfected 293T cells with hemagglutinin-tagged (HA-tagged) GATA-1 and/or Flag-tagged MEK1. Total cellular lysates were prepared after 36 h, and GATA-1 was immunoprecipitated with the anti-HA Ab and MEK1 with the anti-Flag Ab. As shown in Fig. 4*D*, immunoblotting with the anti-Flag Ab showed that MEK1 was coimmunoprecipitated with GATA-1 only when both molecules were cotransduced. Also, immunoblotting with the anti-HA Ab showed that GATA-1 was coimmunoprecipitated with MEK1.

Next, to examine whether endogenous GATA-1 and MEK interact in primary erythroid cells, we performed a coimmunoprecipitation analysis using murine BM erythroid cells: Cells positive for CD71 (transferrin receptor), which is expressed at high levels on erythroid progenitors, were purified using the MACS immunomagnetic separation system. Total cellular lysate was prepared and subjected to immunoprecipitation with an anti-GATA-1 Ab or rat isotype IgG. Fig. 4*E* shows that MEK is coimmunoprecipitated with GATA-1, indicating that these molecules actually interact with each other in primary erythroid cells.

Finally, we investigated whether MEK1 directly binds to GATA-1 *in vitro* by GST pull-down assays. After verifying the quality and quantity of GST-MEK1 fusion protein by Coomassie Brilliant Blue staining (data not shown), we analyzed the binding between GST-MEK1 and *in vitro*-translated GATA-1. As shown in Fig. 4*F*, GST-MEK1 but not GST alone, bound to ^{35}S-labeled GATA-1 *in vitro*.

Together with the results of Fig. 4, *A–C*, we proved the following two facts: GATA-1 inhibits MEK activation; GATA-1 and MEK interact with each other in primary erythroid progenitors. From these facts, we speculated that GATA-1 blocks Ras signal at least partly through the direct interaction with MEK1.

Oncogenic Ras Induces Suppression of Erythropoiesis through the Induction of p21$^{CIP1/WAF1}$—In addition to the functions to deliver mitogenic and anti-apoptotic signals (14), Ras paradoxically causes growth arrest (senescence) in normal cells through several cell cycle regulatory molecules such as p53, p16^{INK4a}, p19^{ARF}, and p21$^{CIP1/WAF1}$ (15, 21). Among them, p53 is a tumor-suppressor and acts as a pivotal regulator of these responses (15, 16, 19, 21). p19^{ARF} is a splicing variant of p16^{INK4a} and inhibits the function of H/MDM2, which pro-

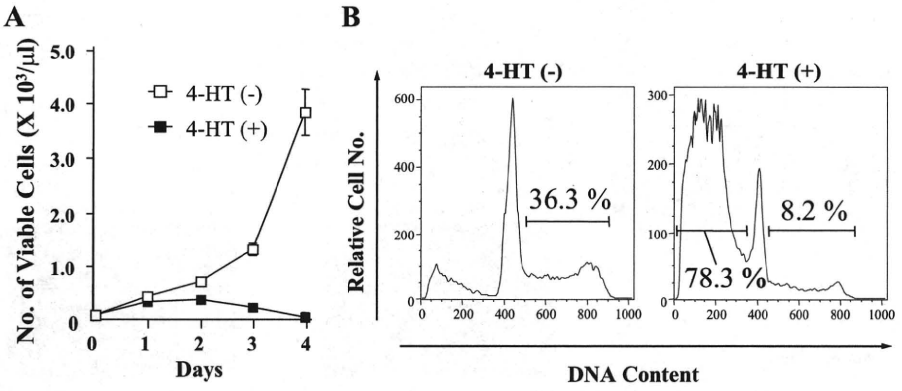

FIGURE 3. **Inhibition of Ras-dependent cell proliferation and survival by GATA-1.** *A*, Ba/F3/N-RasE12/G1ERT cells were seeded at a density of 100/μl and cultured in RPMI supplemented with 1% FBS without IL-3 in the presence or absence of 1 μM 4-HT. Total numbers of viable cells were counted by trypan blue dye exclusion method on the indicated days. The results are shown as means ± S.D. of triplicate cultures. *B*, after 48 h of culture, DNA contents of 4-HT-treated or untreated cells were examined by propidium iodide staining. The proportions of cells in S-G2/M phase and subdiploid fraction are shown, respectively.

motes degradation of p53 (30). p16^{INK4a} is a member of the INK4 family of CDK inhibitors, which causes cell cycle arrest at G1 phase by inhibiting CDK4/6 activities (30). Meanwhile, p21$^{CIP1/WAF1}$ is a member of the Cip/Kip family of CDK inhibitors and also induces G1 arrest by inhibiting CDK2 activities. In this report, we next examined their roles in N-RasE12-induced suppression of erythropoiesis.

At first, we examined the effects of N-RasE12 on the expression of p16^{INK4a}, p19^{ARF}, and p21$^{CIP1/WAF1}$ by semiquantitative/real-time RT-PCR analyses or immunofluorescence. As shown in Fig. 5*A* and *B*, the expression of p16^{INK4a} and p19^{ARF} was induced in N-RasE12-transduced LSK cells both in mRNA and protein levels. Also, the expression of p21$^{CIP1/WAF1}$ was increased by nearly 2-fold in N-RasE12-transduced LSK cells compared with mock-transduced LSK cells (Fig. 5*C*), suggesting that the up-regulated p16^{INK4a}, p19^{ARF}, and/or p21$^{CIP1/WAF1}$ might be involved in N-RasE12-induced suppression of erythropoiesis.

To further analyze the roles of these molecules, we next introduced N-RasE12 into LSK cells isolated from p16^{INK4a}/p19^{ARF} double knock-out (KO) mice, cocultured them with MS-5, and examined the development of erythroid cells by flow cytometry. As shown in Fig. 6*A*, the frequency of CD45^{low}TER-119^{+} erythroid cells was a little lower in N-RasE12-transduced double KO cells than in N-RasE12-transduced WT cells (WT 1.8% *versus* double KO 0.8%) (*upper panels*). In addition, although the number of these erythroid cells was slightly restored in N-RasE12-transduced double KO cells compared with N-RasE12-transduced WT cells (*lower graph*), this difference was not significant.

We also introduced N-RasE12 into LSK cells isolated from p21$^{CIP1/WAF1}$-null mice. As observed in the other experiments, N-RasE12 reduced the proportion of CD45^{low}TER-119^{+} erythroid cells both in WT and p21$^{CIP1/WAF1}$-null LSK cells (Fig. 6*B*, *upper panels*). However, p21$^{CIP1/WAF1}$ deficiency partially, but significantly, restored the proportion of this fraction from 3.0 to 5.2%. In addition, surprisingly, N-RasE12 increased the number of erythroid cells in p21$^{CIP1/WAF1}$-null LSK cells compared with mock-transduced LSK cells (Fig. 6*C*, *lower graph*), indicating that p21$^{CIP1/WAF1}$ is a major regulator of N-RasE12-induced suppression of erythropoiesis.

Because the expression of p21$^{CIP1/WAF1}$ is regulated in p53-dependent and independent manners (31–33), we finally investigated the roles of p53 in N-RasE12-induced suppression of erythropoiesis with the similar experiment. As shown in Fig. 6*C*, the proportion and number of erythroid cells in mock-transduced LSK cells were reduced by p53 deficiency. In addition, p53 deficiency did not cancel the inhibition of erythroid cell development by N-RasE12. Together, these results indicate that N-RasE12 inhibits erythropoiesis through p21$^{CIP1/WAF1}$ in a p53-independent manner.

DISCUSSION

We here found that BCR-ABL suppresses erythroid cell proliferation. This finding is largely consistent with clinical features of CML, in which anemia is commonly observed and erythroid blast crisis is a rare event. Also, we found that constitutively activated Ras, but not PI3-K or STAT5, inhibits erythropoiesis and that a farnesyltransferase inhibitor, manumycin A, restores erythroid colony formation of CML patients BM cells at relatively low concentrations. These results strongly indicate that Ras is a negative regulator of erythropoiesis downstream of BCR-ABL. So far, functions of Ras in normal erythropoiesis are controversial. It was reported that Ras signaling was essential for development of erythroid progenitors (34, 35). In contrast, H-Ras$^{-/-}$, N-Ras$^{-/-}$, and double KO (H-Ras$^{-/-}$ N-Ras$^{-/-}$) mice had no apparent hematopoietic abnormality, indicating that Ras is dispensable for normal erythropoiesis (36, 37). Regarding the roles of oncogenic Ras in erythropoiesis, it was shown that oncogenic H-Ras blocks terminal erythroid differentiation (38), and that enforced expression of an active mutant of N-Ras in primitive hematopoietic cells inhibits proliferation of erythroid cells (17, 18). Our results indicate that the excessive Ras signal would inhibit erythropoiesis, though Ras signal might be to some extent necessary for erythroid cell survival. Ras is mutated in a significant proportion of cases with acute myeloid leukemia and myelodysplastic syndromes (39), or constitutively activated by various oncogenic TKs, including FLT3-ITD (2), c-KIT D816V (40), and TEL-PDGFRB (41). So, anemia observed in these hematologic malignancies also might be, at least partly, attributed to the constitutively activated Ras signal. However, in this study, JAK2 V617F slightly enhanced erythropoiesis as observed in patients with PV, whereas its downstream pathways including Ras, PI3-K, and STAT5 are common to BCR-ABL (1, 5). As for this difference, we here found that JAK2 V617F does not activate Ras signal so strongly as BCR-ABL. Also, it was speculated that JAK2 V617F would utilize mainly STAT5 to promote erythropoiesis in PV patients. Although Ras has some isoforms, we focused on N-Ras,

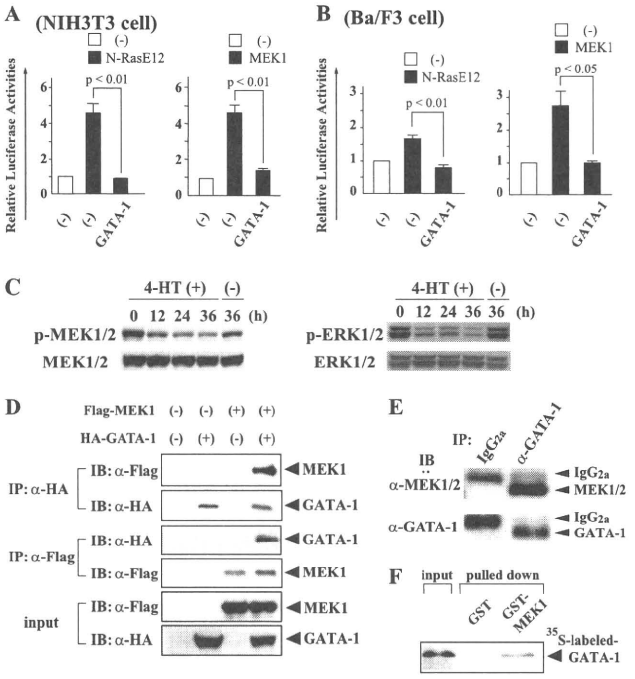

FIGURE 4. **GATA-1 blocks the Ras/Raf/MEK/ERK pathway through its direct interaction with MEK1.** *A*, NIH3T3 cells (2×10^5 cells seeded in 60-mm dish) were transfected with the indicated expression vectors and the reporter gene ($3 \times$ AP-1-Luc) together with pRL-CMV. After 12 h, the cells were serum-deprived for 24 h, then lysed, and subjected to the measurement of the firefly and *Renilla* luciferase activities. The relative firefly luciferase activities normalized by the *Renilla* luciferase activities are shown as means ± S.D. of three separate experiments. *B*, Ba/F3 cells (2×10^6 cells) were transfected with the same vectors as Fig. 4*A* using Amaxa Nucleofector technology. After 24 h of culture, the cells were lysed and subjected to the measurement of the luciferase activities. *C*, Ba/F3/N-RasE12/G1ERT cells cultured in RPMI supplemented with 1% FBS were treated with 1 μM 4-HT or vehicle. Total cellular lysates were prepared at the indicated time and subjected to immunoblotting with the indicated Abs. The filters were reprobed with corresponding Abs to confirm that the equal amounts of the proteins were loaded. *D*, coimmunoprecipitation analyses were performed using 293T cells transfected with HA-tagged GATA-1 and/or Flag-tagged MEK1 as indicated. *IP*, immunoprecipitation; *IB*, immunoblotting; *α*, anti. *E*, total cellular lysate was prepared from murine BM CD71$^+$ cells. Immunoprecipitation and immunoblot analyses were performed with the indicated antibodies. F. The *in vitro* binding between GATA-1 and MEK1 was examined by GST pull-down assays. ^{35}S-labeled GATA-1 was incubated with GST-MEK1 bound to glutathione-Sepharose beads, and the binding complex was separated by gel electrophoresis and subjected to autoradiography.

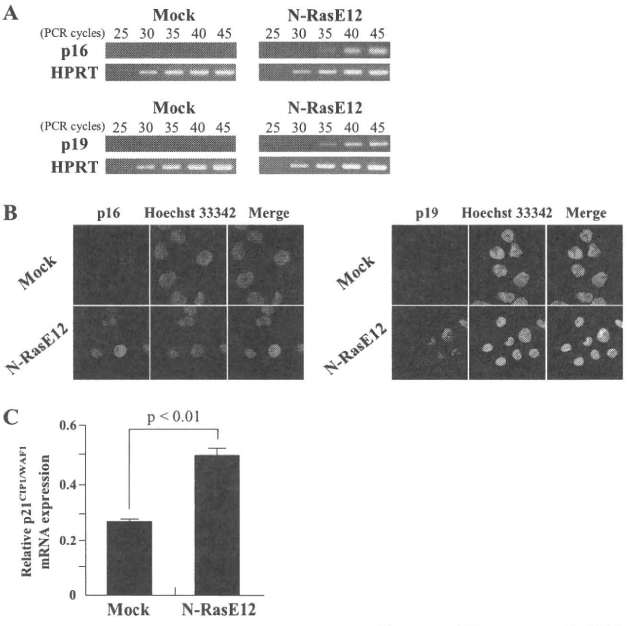

FIGURE 5. **Increase in expression levels of p16^{INK4a}, p19^{ARF}, and p21$^{CIP1/WAF1}$ by oncogenic Ras.** *A–C*, LSK cells transfected with Mock or N-RasE12 were cultured with rmSCF, rmIL-3, and rhEPO for 2 days. Total RNA was isolated from GFP$^+$ cells, and the expression levels of p16^{INK4a} and p19^{ARF} were analyzed by semiquantitative RT-PCR (*A*). Immunofluorescence staining of p16^{INK4a} and p19^{ARF} localizations (*red*) in Hoechst 33342-stained nuclei of GFP$^+$ cells are shown (magnification, 630×) (*B*). The expression levels of p21$^{CIP1/WAF1}$ were analyzed by real-time RT-PCR. The results are normalized to the levels of HPRT gene and shown as means ± S.D. ($n = 3$) (*C*).

because, in myeloid malignancies, N-Ras mutations are more frequent than K-Ras, whereas H-Ras mutations are rare (39, 42–44). It is predictable that activated N-Ras has stronger leukemogenic potential than activated H-Ras or K-Ras.

In contrast to the negative role of oncogenic Ras in erythropoiesis, Ras activation prominently enhanced the development of myeloid cells from LSK cells as observed in CML patients. To clarify the mechanism through which the active form of Ras plays different roles in the growth of hematopoietic cells according to the cell lineages (*i.e.* inhibition of erythropoiesis but promotion of myelopoiesis), we examined the role of GATA-1, which is a transcription factor mainly expressed in erythroid and megakaryocytic cells but not in myeloid cells. Ras-induced suppression of erythropoiesis can be considered to result from inhibition of proliferation of already committed erythroid progenitors, and blockage of commitment into erythroid lineage from HSCs. In this study, we found that GATA-1 inhibits MEK activity and suppresses the Ras-dependent proliferation of GATA-1-posistive cells. GATA-1 is necessary in the post-commitment stages of erythroid and megakaryocytic development, and is highly expressed after the commitment into megakaryocyte-erythrocyte progenitors (MEPs), but is scarcely expressed in HSCs (45). So, it is unlike that the interaction between GATA-1 and MEK1 is associated with the lineage determination of HSCs. On the other hand, recent reports showed that suppression of erythroid cell development by H-, K-, and N-Ras occurs at later stages of differentiation (18, 38, 46). These data are consistent with our result that GATA-1 interacts with MEK1, thereby inhibiting Ras-mediated mitogenic signals.

However, this result raises a question where these molecules interact together in the cells because GATA-1 is located in the nucleus and MEK is in the cytoplasm (47). As an explanation it was previously reported that MEK contains a nuclear export signal in its N-terminal domain, indicating that MEK is translocated to the nucleus upon mitogenic stimulation and then goes back to the cytoplasm after transduction of its signal (48). So, GATA-1 is supposed to interact with MEK1 in the nucleus, thereby inhibiting its activity. This hypothesis that GATA-1 would inhibit MEK activities is also contradictory to the fact that platelet counts are often elevated in CML patients, because MEK has been shown to be important for the maturation (polyploidization) of megakaryocytes, in which GATA-1 is highly expressed as well as in erythroid cells. Regarding this issue, Jacquel *et al.* reported that PMA-induced megakaryocytic maturation is only partly dependent on the MEK/ERK pathway and suggested the involvement of other pathways such

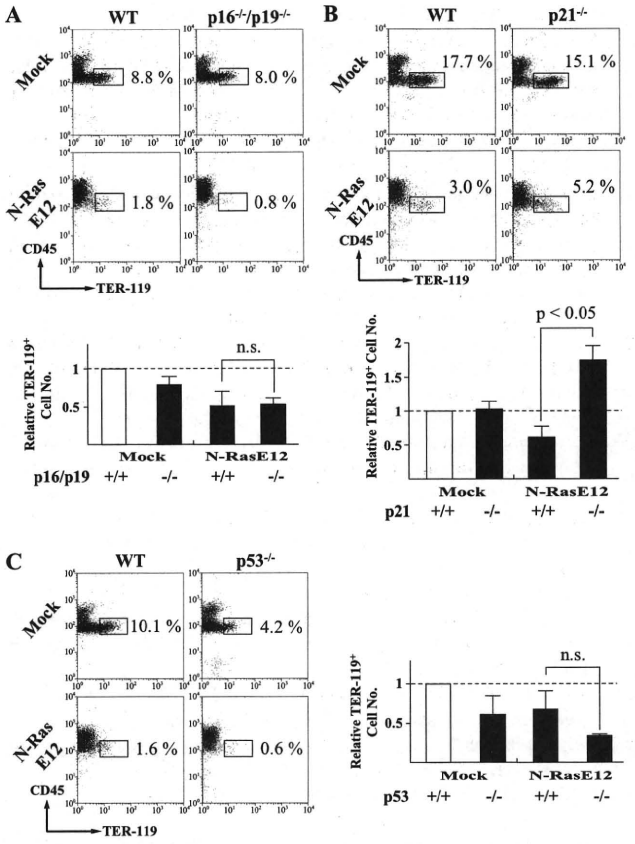

FIGURE 6. **p21$^{CIP1/WAF1}$ but not p53 or p16^{INK4a}/p19^{ARF} mediates oncogenic Ras-induced suppression of erythropoiesis.** *A–C*, LSK cells were isolated from BM of the indicated mice. After retrovirus infection, GFP$^+$ cells were sorted and cocultured with MS-5 in the presence of rmSCF and rhEPO. The expression of CD45 and TER-119 was analyzed after 5 days. Bar graphs represent the relative TER-119$^+$ cell numbers normalized to mock-transduced WT cells (*dashed lines*). *n.s.*, not significant.

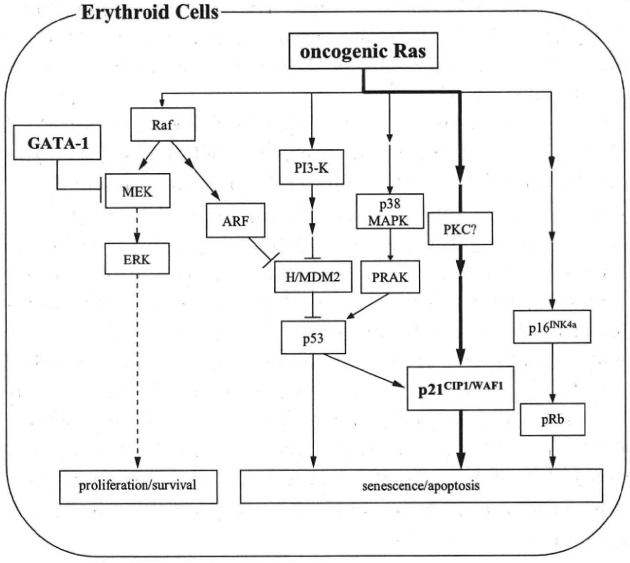

FIGURE 7. **A proposed model for oncogenic Ras-induced suppression of erythropoiesis.** Oncogenic Ras simultaneously activates several downstream molecules including Raf, PI3-K, and p38 MAPK. The Raf/MEK/ERK pathway mainly transduces proliferation and survival signals, while the remaining pathways commonly induce growth arrest (senescence) through cell cycle regulatory molecules such as p16^{INK4a}, p19^{ARF}, p21$^{CIP1/WAF1}$, and p53. So, oncogenic Ras is supposed to induce proliferation or senescence dependently on the balance between these two signals. In this study, we found that GATA-1 inhibits mitogenic signal from Ras through its interaction with MEK1 in erythroid cells, which resulted in their growth inhibition due to the dominance of senescence-inducing signals. In addition, we found that p21$^{CIP1/WAF1}$ is a crucial regulator of oncogenic Ras-induced senescence of erythroid cells.

as Jun N-terminal kinase (JNK) and protein kinase C (PKC) in CML cells (49). Alternatively, it is also possible that the interaction between GATA-1 and MEK might be inhibited in megakaryocytes due to the presence of some nuclear protein(s) specific for this lineage. However, further studies are required to clarify how megakaryocytes develop and platelets are effectively produced in CML patients.

Among various signaling molecules downstream of Ras, the Raf/MEK/ERK pathway mainly promotes cell growth and prevents apoptosis of hematopoietic cells (14). On the other hand, oncogenic stimuli including constitutively activated Ras, also cause growth inhibition (senescence) that acts as a fail-safe mechanism against malignant transformation (15, 16, 21). Although the mechanism of Ras-induced senescence is not fully understood, recent findings have unveiled several MEK/ERK-independent pathways (19). These pathways regulate the function of two main tumor-suppressor molecules, p53 and retinoblastoma protein (pRb) (50). Downstream of oncogenic Ras, p38-regulated/activated protein kinase (PRAK), a substrate of p38 mitogen-activated protein kinase (p38 MAPK), activates p53 by direct phosphorylation (20). Ras/Raf stabilizes p53 independently of MEK through the up-regulation of p19^{ARF} (21). The PI3-K pathway also stabilizes p53 through the inhibition of H/MDM2 (19). So, we speculated that N-RasE12 might induce growth arrest in erythroid cells even if MEK activities are blocked by GATA-1.

Ras-induced senescence is executed by CDK inhibitors such as p16^{INK4a} and p21$^{CIP1/WAF1}$, and a tumor-suppressor, p19^{ARF}, which consequently activate both p53 and pRb pathways. Among these molecules, we here found that p21$^{CIP1/WAF1}$ is a major player of Ras-induced suppression of erythropoiesis (may well be called nearly equal to senescence). Although p21$^{CIP1/WAF1}$ is a transcriptional target of p53 (51), p53 deficiency did not cancel Ras-induced suppression of erythropoiesis. So, p53-independent expression of p21$^{CIP1/WAF1}$ was supposed to be important for Ras-induced suppression of erythropoiesis. Because Darley *et al.* (18) previously showed that oncogenic N-Ras conferred developmental abnormalities on human erythroid cells through the activation of PKC, one of the reported activators of p21$^{CIP1/WAF1}$ (52), PKC may be a candidate molecule involved in Ras-induced expression of p21$^{CIP1/WAF1}$ and consequent suppression of erythropoiesis.

Mutation and/or deletion of the p53 gene and the INK4a/ARF locus are frequently observed in CML blast phase (1), but to our knowledge, there is no report demonstrating the inactivation of the p21$^{CIP1/WAF1}$ gene. So, our findings that p21$^{CIP1/WAF1}$ but not p53 or p16^{INK4a}/p19^{ARF} is the major regulator of Ras-induced suppression of erythropoiesis are again consistent with the clinical features that anemia is continued and erythroid transformation is a rare event in blast-phase

CML (7, 8). Furthermore, because loss-of-function mutations of the p21$^{CIP1/WAF1}$ gene are rare in most of the hematologic malignancies, anemia observed in these diseases might be attributable to p21$^{CIP1/WAF1}$.

In conclusion, we here show that BCR-ABL but not JAK2 V617F inhibits erythropoiesis through the Ras signal. We also identified p21$^{CIP1/WAF1}$ as a central regulator of Ras-induced suppression of erythropoiesis. Ras transmits both growth promoting and inhibitory signals, and then induces proliferation or senescence dependently on their balance. In erythroid but not in myeloid progenitors, the growth promoting signal is inhibited at the level of MEK by GATA-1, which would lead to the relative dominance of the growth inhibitory signal mediated by p21$^{CIP1/WAF1}$ (Fig. 7). These mechanisms would explain why oncogenic Ras simultaneously reveals conflicting effects according to the cell lineage, *i.e.* growth promotion in myeloid cells and growth inhibition in erythroid cells. This model may be also useful to understand the mechanism of anemia caused by other oncogenic TKs.

Acknowledgments—We thank Dr. Connie J. Eaves for providing the vector expressing p210-BCR-ABL, Dr. Kazuya Shimoda for providing the plasmid encoding JAK2 V617F, and Dr. Hiroyuki Miyoshi for providing 293gp cells.

REFERENCES

1. Quintás-Cardama, A., and Cortes, J. (2009) *Blood* **113,** 1619–1630
2. Small, D. (2006) *Hematology Am. Soc. Hematol. Educ. Program*, 178–184
3. Levine, R. L., and Gilliland, D. G. (2008) *Blood* **112,** 2190–2198
4. Ren, R. (2005) *Nat. Rev. Cancer* **5,** 172–183
5. Zeuner, A., Pedini, F., Signore, M., Ruscio, G., Messina, C., Tafuri, A., Girelli, G., Peschle, C., and De Maria, R. (2006) *Blood* **107,** 3495–3502
6. Thiele, J., Kvasnicka, H. M., Schmitt-Graeff, A., Zirbes, T. K., Birnbaum, F., Kressmann, C., Melguizo-Grahmann, M., Frackenpohl, H., Sprungmann, C., Leder, L. D., Diehl, V., Zankovich, R., Schaefer, H. E., Niederle, N., and Fischer, R. (2000) *Leuk. Lymphoma* **36,** 295–308
7. Saikia, T., Advani, S., Dasgupta, A., Ramakrishnan, G., Nair, C., Gladstone, B., Kumar, M. S., Badrinath, Y., and Dhond, S. (1988) *Leuk. Res.* **12,** 499–506
8. Griffin, J. D., Todd, R. F., 3rd, Ritz, J., Nadler, L. M., Canellos, G. P., Rosenthal, D., Gallivan, M., Beveridge, R. P., Weinstein, H., Karp, D., and Schlossman, S. F. (1983) *Blood* **61,** 85–91
9. Sonoyama, J., Matsumura, I., Ezoe, S., Satoh, Y., Zhang, X., Kataoka, Y., Takai, E., Mizuki, M., Machii, T., Wakao, H., and Kanakura, Y. (2002) *J. Biol. Chem.* **277,** 8076–8082
10. Sexl, V., Piekorz, R., Moriggl, R., Rohrer, J., Brown, M. P., Bunting, K. D., Rothammer, K., Roussel, M. F., and Ihle, J. N. (2000) *Blood* **96,** 2277–2283
11. Hoelbl, A., Kovacic, B., Kerenyi, M. A., Simma, O., Warsch, W., Cui, Y., Beug, H., Hennighausen, L., Moriggl, R., and Sexl, V. (2006) *Blood* **107,** 4898–4906
12. Sawyers, C. L., McLaughlin, J., and Witte, O. N. (1995) *J. Exp. Med.* **181,** 307–313
13. Baum, K. J., and Ren, R. (2008) *J. Hematol. Oncol.* **1,** 5
14. Platanias, L. C. (2003) *Blood* **101,** 4667–4679
15. Campisi, J. (2005) *Cell* **120,** 513–522
16. Braig, M., and Schmitt, C. A. (2006) *Cancer Res.* **66,** 2881–2884
17. Darley, R. L., Hoy, T. G., Baines, P., Padua, R. A., and Burnett, A. K. (1997) *J. Exp. Med.* **185,** 1337–1347
18. Darley, R. L., Pearn, L., Omidvar, N., Sweeney, M., Fisher, J., Phillips, S., Hoy, T., and Burnett, A. K. (2002) *Blood* **100,** 4185–4192
19. Yaswen, P., and Campisi, J. (2007) *Cell* **128,** 233–234
20. Sun, P., Yoshizuka, N., New, L., Moser, B. A., Li, Y., Liao, R., Xie, C., Chen, J., Deng, Q., Yamout, M., Dong, M. Q., Frangou, C. G., Yates, J. R., 3rd, Wright, P. E., and Han, J. (2007) *Cell* **128,** 295–308
21. Wahl, G. M., and Carr, A. M. (2001) *Nat. Cell Biol.* **3,** E277–286
22. Ezoe, S., Matsumura, I., Gale, K., Satoh, Y., Ishikawa, J., Mizuki, M., Takahashi, S., Minegishi, N., Nakajima, K., Yamamoto, M., Enver, T., and Kanakura, Y. (2005) *J. Biol. Chem.* **280,** 13163–13170
23. Delgado, M. D., Vaqué, J. P., Arozarena, I., López-Ilasaca, M. A., Martínez, C., Crespo, P., and León, J. (2000) *Oncogene* **19,** 783–790
24. Onishi, M., Nosaka, T., Misawa, K., Mui, A. L., Gorman, D., McMahon, M., Miyajima, A., and Kitamura, T. (1998) *Mol. Cell. Biol.* **18,** 3871–3879
25. Egawa, K., Sharma, P. M., Nakashima, N., Huang, Y., Huver, E., Boss, G. R., and Olefsky, J. M. (1999) *J. Biol. Chem.* **274,** 14306–14314
26. Jiang, X., Ng, E., Yip, C., Eisterer, W., Chalandon, Y., Stuible, M., Eaves, A., and Eaves, C. J. (2002) *Blood* **100,** 3731–3740
27. Shide, K., Shimoda, H. K., Kumano, T., Karube, K., Kameda, T., Takenaka, K., Oku, S., Abe, H., Katayose, K. S., Kubuki, Y., Kusumoto, K., Hasuike, S., Tahara, Y., Nagata, K., Matsuda, T., Ohshima, K., Harada, M., and Shimoda, K. (2008) *Leukemia* **22,** 87–95
28. Matsumura, I., Kanakura, Y., Kato, T., Ikeda, H., Horikawa, Y., Ishikawa, J., Kitayama, H., Nishiura, T., Tomiyama, Y., Miyazaki, H., and Matsuzawa, Y. (1996) *Blood* **88,** 3074–3082
29. Fukushima, K., Matsumura, I., Ezoe, S., Tokunaga, M., Yasumi, M., Satoh, Y., Shibayama, H., Tanaka, H., Iwama, A., and Kanakura, Y. (2009) *J. Biol. Chem.* **284,** 7719–7732
30. Roussel, M. F. (1999) *Oncogene* **18,** 5311–5317
31. el-Deiry, W. S., Tokino, T., Velculescu, V. E., Levy, D. B., Parsons, R., Trent, J. M., Lin, D., Mercer, W. E., Kinzler, K. W., and Vogelstein, B. (1993) *Cell* **75,** 817–825
32. Macleod, K. F., Sherry, N., Hannon, G., Beach, D., Tokino, T., Kinzler, K., Vogelstein, B., and Jacks, T. (1995) *Genes Dev.* **9,** 935–944
33. Parker, S. B., Eichele, G., Zhang, P., Rawls, A., Sands, A. T., Bradley, A., Olson, E. N., Harper, J. W., and Elledge, S. J. (1995) *Science* **267,** 1024–1027
34. Khalaf, W. F., White, H., Wenning, M. J., Orazi, A., Kapur, R., and Ingram, D. A. (2005) *Blood* **105,** 3538–3541
35. Sui, X., Krantz, S. B., You, M., and Zhao, Z. (1998) *Blood* **92,** 1142–1149
36. Esteban, L. M., Vicario-Abejón, C., Fernández-Salguero, P., Fernández-Medarde, A., Swaminathan, N., Yienger, K., Lopez, E., Malumbres, M., McKay, R., Ward, J. M., Pellicer, A., and Santos, E. (2001) *Mol. Cell. Biol.* **21,** 1444–1452
37. Umanoff, H., Edelmann, W., Pellicer, A., and Kucherlapati, R. (1995) *Proc. Natl. Acad. Sci. U.S.A.* **92,** 1709–1713
38. Zhang, J., Socolovsky, M., Gross, A. W., and Lodish, H. F. (2003) *Blood* **102,** 3938–3946
39. MacKenzie, K. L., Dolnikov, A., Millington, M., Shounan, Y., and Symonds, G. (1999) *Blood* **93,** 2043–2056
40. Metcalfe, D. D. (2008) *Blood* **112,** 946–956
41. Wheadon, H., and Welham, M. J. (2003) *Blood* **102,** 1480–1489
42. Döhner, K., and Döhner, H. (2008) *Haematologica* **93,** 976–982
43. Neubauer, A., Greenberg, P., Negrin, R., Ginzton, N., and Liu, E. (1994) *Leukemia* **8,** 638–641
44. Flotho, C., Valcamonica, S., Mach-Pascual, S., Schmahl, G., Corral, L., Ritterbach, J., Hasle, H., Aricò, M., Biondi, A., and Niemeyer, C. M. (1999) *Leukemia* **13,** 32–37
45. Akashi, K., Traver, D., Miyamoto, T., and Weissman, I. L. (2000) *Nature* **404,** 193–197
46. Zhang, J., Liu, Y., Beard, C., Tuveson, D. A., Jaenisch, R., Jacks, T. E., and Lodish, H. F. (2007) *Blood* **109,** 5238–5241
47. Lenormand, P., Sardet, C., Pagès, G., L'Allemain, G., Brunet, A., and Pouysségur, J. (1993) *J. Cell Biol.* **122,** 1079–1088
48. Jaaro, H., Rubinfeld, H., Hanoch, T., and Seger, R. (1997) *Proc. Natl. Acad. Sci. U.S.A.* **94,** 3742–3747
49. Jacquel, A., Herrant, M., Defamie, V., Belhacene, N., Colosetti, P., Marchetti, S., Legros, L., Deckert, M., Mari, B., Cassuto, J. P., Hofman, P., and Auberger, P. (2006) *Oncogene* **25,** 781–794
50. Serrano, M., Lin, A. W., McCurrach, M. E., Beach, D., and Lowe, S. W. (1997) *Cell* **88,** 593–602
51. Deng, Y., Chan, S. S., and Chang, S. (2008) *Nat. Rev. Cancer* **8,** 450–458
52. Biggs, J. R., Kudlow, J. E., and Kraft, A. S. (1996) *J. Biol. Chem.* **271,** 901–906

THE JOURNAL OF BIOLOGICAL CHEMISTRY VOL. 284, NO. 12, pp. 7719–7732, March 20, 2009

FIP1L1-PDGFRα Imposes Eosinophil Lineage Commitment on Hematopoietic Stem/Progenitor Cells*

Received for publication, September 26, 2008, and in revised form, December 22, 2008 Published, JBC Papers in Press, January 14, 2009, DOI 10.1074/jbc.M807489200

Kentaro Fukushima[‡], Itaru Matsumura[‡], Sachiko Ezoe[‡§1], Masahiro Tokunaga[‡], Masato Yasumi[‡], Yusuke Satoh[‡], Hirohiko Shibayama[‡], Hirokazu Tanaka[‡], Atsushi Iwama[¶], and Yuzuru Kanakura[‡]

From the [‡]Department of Hematology and Oncology, Osaka University Graduate School of Medicine, 2-2, Yamada-oka, Suita, Osaka 565-0871, Japan, the [§]Medical Center of Translational Research, Osaka University Hospital, Suita, Osaka 565-0871, Japan, and [¶]Cellular and Molecular Medicine, Graduate School of Medicine, Chiba University, Chiba 260-8670, Japan

Although leukemogenic tyrosine kinases (LTKs) activate a common set of downstream molecules, the phenotypes of leukemia caused by LTKs are rather distinct. Here we report the molecular mechanism underlying the development of hypereosinophilic syndrome/chronic eosinophilic leukemia by FIP1L1-PDGFRα. When introduced into c-Kit^{high}Sca-1^{+}Lineage^{-} cells, FIP1L1-PDGFRα conferred cytokine-independent growth on these cells and enhanced their self-renewal, whereas it did not immortalize common myeloid progenitors in *in vitro* replating assays and transplantation assays. Importantly, FIP1L1-PDGFRα but not TEL-PDGFRβ enhanced the development of Gr-1^{+}IL-5Rα^{+} eosinophil progenitors from c-Kit^{high}Sca-1^{+}Lineage^{-} cells. FIP1L1-PDGFRα also promoted eosinophil development from common myeloid progenitors. Furthermore, when expressed in megakaryocyte/erythrocyte progenitors and common lymphoid progenitors, FIP1L1-PDGFRα not only inhibited differentiation toward erythroid cells, megakaryocytes, and B-lymphocytes but aberrantly developed eosinophil progenitors from megakaryocyte/erythrocyte progenitors and common lymphoid progenitors. As for the mechanism of FIP1L1-PDGFRα-induced eosinophil development, FIP1L1-PDGFRα was found to more intensely activate MEK1/2 and p38^{MAPK} than TEL-PDGFRβ. In addition, a MEK1/2 inhibitor and a p38^{MAPK} inhibitor suppressed FIP1L1-PDGFRα-promoted eosinophil development. Also, reverse transcription-PCR analysis revealed that FIP1L1-PDGFRα augmented the expression of *C/EBPα*, *GATA-1*, and *GATA-2*, whereas it hardly affected *PU.1* expression. In addition, short hairpin RNAs against *C/EBPα* and *GATA-2* and *GATA-3KRR*, which can act as a dominant-negative form over all GATA members, inhibited FIP1L1-PDGFRα-induced eosinophil development. Furthermore, FIP1L1-PDGFRα and its downstream Ras inhibited PU.1 activity in luciferase assays. Together, these results indicate that FIP1L1-PDGFRα enhances eosinophil development by modifying the expression and activity of lineage-specific transcription factors through Ras/MEK and p38^{MAPK} cascades.

During the last decade, it has become clear that hematopoietic growth factors regulate only growth and survival of hematopoietic cells, whereas lineage-specific transcription factors, such as GATA-1, GATA-3, PU.1, Pax-5, C/EBPα, and C/EBPε, crucially control the lineage commitment and lineage-specific differentiation. For example, granulocyte colony-stimulating factor signaling induced megakaryopoiesis in granulocyte colony-stimulating factor receptor-transgenic mice (1). Also, erythropoietin (EPO)[2] was found to promote terminal granulocytic differentiation in EPO receptor-transgenic mice. From these data, we speculated that signal transduction molecules activated by hematopoietic growth factors would not influence the lineage commitment of hematopoietic stem cells/progenitor cells (HSCs/HPCs) or subsequent lineage-specific differentiation (2). However, it has very recently been shown that the MEK/ERK pathway is involved in myeloid lineage commitment (3). Also, PKB (c-Akt) was shown to be involved in lineage decision during myelopoiesis (4). In addition, FLT3-activating mutations were proved to inhibit C/EBPα activity through ERK1/2-mediated phosphorylation (3, 5). These results suggest that signal transduction molecules activated by hematopoietic growth factors or their genetic mutations would not only promote growth and survival but also influence lineage commitment and subsequent differentiation of hematopoietic cells.

Activating mutations of the tyrosine kinases (TKs), such as c-Kit, platelet-derived growth factor receptor (PDGFR), FLT3, and c-ABL, are provoked by several mechanisms, including chromosomal translocations and various mutations involving their self-regulatory regions. These mutations are often involved in the pathogenesis of various types of hematologic malignancies. BCR-ABL is known to cause chronic myelogenous leukemia and acute lymphoblastic leukemia. Most patients with *PDGFRβ* rearrangement reveal common clinical

* This work was supported by grants from the Ministry of Education, Science, Sports, and Culture and Technology of Japan. The costs of publication of this article were defrayed in part by the payment of page charges. This article must therefore be hereby marked "*advertisement*" in accordance with 18 U.S.C. Section 1734 solely to indicate this fact.

[1] To whom correspondence should be addressed: Dept. of Hematology and Oncology, Osaka University Graduate School of Medicine, 2-2, Yamada-oka, Suita, Osaka 565-0871, Japan. Tel.: 81-6-6879-3871; Fax: 81-6-6879-3879; E-mail: sezoe@bldon.med.osaka-u.ac.jp.

[2] The abbreviations used are: EPO, erythropoietin; LTK, leukemogenic tyrosine kinase; PDGFRα, platelet-derived factor receptor α; PDGFRβ, platelet-derived factor receptor β; KSL, Lin^{-}Sca^{-}1^{hi}c-Kit^{hi} cell; CMP, common myeloid progenitor; CLP, common lymphoid progenitor; GMP, common granulocyte/monocyte progenitor; HSC, hematopoietic stem cell; HPC, hematopoietic progenitor cell; C/EBP, CCAAT/enhancer-binding protein; MPD, myeloproliferative disorder; TK, tyrosine kinase; AML, acute myeloid leukemia; MAPK, mitogen-activated protein kinase; STAT, signal transducers and activators of transcription; HES, hypereosinophilic syndrome; CEL, chronic eosinophilic leukemia; ERK, extracellular signal-regulated kinase; LSC, leukemic stem cell; MEP, megakaryocyte/erythroid progenitor; FACS, fluorescence-activated cell sorter; shRNA, short hairpin RNA; RT, reverse transcription; GFP, green fluorescent protein; MEK, mitogen-activated protein kinase/extracellular signal-regulated kinase kinase.

features resembling chronic myelogenous leukemia or choronic myelomonocytic leukemia. In contrast, *FLT3* mutations (ITD and point mutations in the TK domain) are primarily detectable in acute myeloid leukemia (AML) or myelodysplastic syndrome (6–8). Also, c-*KIT* mutations in the TK domain (Asp^{816} → Val, Tyr, Phe, or His) are found in patients with aggressive mastocytosis, myelodysplastic syndrome, and AML (9–15). Although these leukemogenic TKs (LTKs) activate a common set of downstream signaling molecules, such as Ras/MAPK, PI3-K/Akt/mTOR, and STATs, the mechanisms by which LTKs cause different disease phenotypes remain to be clarified.

FIP1L1-PDGFRα is a fusion gene, which was originally identified in the patients with hypereosinophilic syndrome (HES)/chronic eosinophilic leukemia (CEL) (16, 17). FIP1L1-PDGFRα fusion protein supports cytokine-independent growth and survival of hematopoietic cells as a constitutively active TK (16, 18–21). As for the downstream signaling molecules, FIP1L1-PDGFRα was shown to activate STAT5, phosphatidylinositol 3-kinase, and Ras/ERK pathways like other LTKs, such as BCR-ABL, TEL-ABL, TEL-JAK2, and TEL-PDGFRβ (18). In addition, Buitenhuis *et al.* (22) recently reported that activation of phosphatidylinositol 3-kinase, ERK1/2, and STAT5 is pivotal for FIP1L1/PDGFRα-induced myeloproliferation.

The concept of "cancer stem cell" has widely been recognized and validated in various types of cancers, including breast cancer, brain tumors, colon cancer, lung cancer, and malignant melanoma. This concept was originally established in AML as a "leukemic stem cell (LSC)" (23, 24). In this concept, LSCs are defined as specific leukemic cells that can cause leukemia when transplanted into NOD/SCID mice. In AML, although leukemic blasts often display relatively homogenous features, they are organized in a hierarchy. Among them, LSCs reveal the most immature $CD34^+CD38^-$ phenotype similar to normal HSCs, whereas several antigen expressions are different. LSCs, which account for only 0.2–1.0% of AML cells in the bone marrow (BM), have both abilities to self-renew and to produce restrictedly differentiated leukemia cells, thereby maintaining themselves and yielding leukemia cells composing the majority (23, 25, 26). It is still unclear whether LSCs originate solely from HSCs or are generated from nonstem immature cells that have acquired *de novo* self-renewal ability. It has been shown that, although common myeloid progenitors (CMPs) and granulocyte/monocyte progenitors (GMPs) have very limited life spans, several leukemogenic oncogenes, such as *MLL-ENL*, *MOZ-TIF2*, and *MLL-AF9*, have an ability to immortalize these cells, thereby enabling them to act as LSCs (27, 28). On the other hand, although LSCs in a chronic phase of chronic myelogenous leukemia are at an HSC level, chronic myelogenous leukemia cells at a CMP/GMP level can act as LSCs in an accelerated phase, suggesting that additional gene mutations can change the main LSC population during disease progression. From these findings, it is now speculated that the leukemia phenotype is determined by the biologic property of the mutated gene and/or the lineage and the differentiation state of LSCs.

In an attempt to analyze the molecular mechanisms by which each LTK causes leukemia with the specific phenotype, we introduced FIP1L1-PDGFRα, which plays a causal role in HES/CEL, into murine HSCs and various types of HPCs. As a result, we found that FIP1L1-PDGFRα specifically enhanced eosinophil development from HSCs/HPCs and imposed the lineage conversion to eosinophil lineage on megakaryocyte/erythroid progenitors (MEPs) and common lymphoid progenitors (CLPs) through Ras/MEK and $p38^{MAPK}$ cascades by modifying the expression and activity of lineage-specific transcription factors.

EXPERIMENTAL PROCEDURES

Reagents and Antibodies—Recombinant human TPO was provided by Kirin Brewery (Tokyo, Japan). Recombinant human FLT3L, human IL-6, murine SCF, murine IL-5, murine IL-7, murine granulocyte-macrophage colony-stimulating factor, and human EPO were purchased from Peprotech (Hamburg, Germany).

Antibodies, Cell Staining, and Sorting—To isolate KSLs and CLPs, murine BM cells were stained with phycoerythrin-conjugated anti-IL-7Rα chain (SB/199) (eBioscience, San Diego, CA), fluorescein isothiocyanate-conjugated anti-Sca-1 (E13-161-7), and APC-conjugated anti-c-Kit (2B8) monoclonal antibodies, and biotinylated rat antibodies specific for the lineage markers Ter119, CD3ε (145-2C11), B220 (RA3–6B2), and Gr-1 (RB6-8C5), followed by staining with streptavidin-PerCP/Cy5.5 (BD Biosciences). Then KSLs and CLPs were sorted as $IL\text{-}7R\alpha^-Lin^-Sca^-1^{hi}c\text{-}Kit^{hi}$ and $IL\text{-}7R\alpha^+Lin^-Sca\text{-}1^{lo}c\text{-}Kit^{lo}$ populations, respectively. For myeloid progenitor sorting, murine BM cells were stained with phycoerythrin-conjugated anti-FcγRII/III (2.4G2), fluorescein isothiocyanate-conjugated anti-CD34 (RAM34) (BD Biosciences), APC-conjugated anti-c-Kit, biotinylated anti-Sca-1, and anti-IL-7Rα (SB/199) (Serotec, Raleigh, NC) monoclonal antibodies, and the above described lineage mixture of monoclonal antibodies (BD Biosciences), followed by staining with avidin-APC/Cy7 (BD Biosciences). After the staining, $IL\text{-}7R\alpha^-Lin^-Sca\text{-}1^-c\text{-}Kit^+CD34^+Fc\gamma RII/III^{lo}$ were sorted as CMPs, $IL\text{-}7R\alpha^-Lin^-Sca\text{-}1^-c\text{-}Kit^+CD34^+Fc\gamma RII/III^{hi}$ as GMPs, and $IL\text{-}7R\alpha^-Lin^-Sca\text{-}1^-c\text{-}Kit^+CD34^-Fc\gamma RII/III^{lo}$ as MEPs, as described previously (29). All of these HSCs and HPCs were isolated using a FACS Aria (BD Bioscience, San Jose, CA). In all analyses and sorting, dead cells were excluded by staining with 7-amino-actinomycin D (Calbiochem). Cells were stained with phycoerythrin-conjugated CD125 (IL-5 receptor α-subunit, T21) and APC-conjugated Gr-1(RB6–8C5) (BD Biosciences) for detection of eosinophil lineage.

Plasmids—Expression vectors for FIP1L1-PDGFRα and TEL-PDGFRβ were kindly provided by Dr. D. Gary Gilliland (Harvard Medical School, Boston, MA). Expression vectors for PDGFRα V561D and D842V were kindly provided by Dr. S. Hirota (Hyogo Medical School, Hyogo, Japan). *FIP1L1-PDGFRα*, *TEL-PDGFRβ*, *PDGFRαV561D*, and *PDGFRαD842V* were cloned into the murine stem cell virus-internal ribosome entry site-EGFP (pMie) vector. Also, we constructed *FIP1L1-PDGFRβ* and *TEL-PDGFRα* by the PCR method and subcloned them into pMie.

Short hairpin RNA (shRNA) interference oligonucleotides against GATA-2 and C/EBPα described previously (30, 31) were cloned into an shRNA expression vector, pCS-RfA-CG, which was kindly provided by Dr. Miyoshi H (RIKEN Bio-

Resource center, Tsukuba, Japan). The retrovirus expression vector for dominant negative GATA was constructed by cloning human *GATA-3KRR* cDNA that can inhibit GATA-1, GATA-2, and GATA-3 (32) into pMie.

Cell Culture and Preparation—Murine BM cells were obtained from 6–8-week-old C57BL/6J mice, which were purchased from CLEA (Tokyo, Japan). After sedimentation of the red blood cells with 6% hydroxyethyl starch, mononuclear cells were separated by density gradient centrifugation, using HISTOPAQUE 1083 (Sigma). KSLs, CMPs, GMPs, and MEPs were purified from mononuclear cells and cultured in RPMI1641 medium (Nacalai Tesque, Kyoto, Japan) supplemented with 10% fetal calf serum (EQUITECH-BIO, Kerrville, TX) in the presence of murine SCF (50 ng/ml), human FLT3L (10 ng/ml), human IL-6 (50 ng/ml), and human TPO (50 ng/ml) for 48 h, and the cells were subjected to the retrovirus infection.

Retrovirus Transduction—The conditioned media containing high titer retrovirus particles were prepared as described previously (33). Briefly, an ecotropic packaging cell line, 293gp, kindly provided by Dr. H. Miyoshi (RIKEN BioResource Center, Tsukuba, Japan), was transfected with each retrovirus vector by the calcium phosphate coprecipitation method. After 12 h, the cells were washed and cultured for 48 h. To produce lentivirus, 293T cells were transfected with each shRNA expression vector together with a packaging vector (pCAG-HIVgp) and a lentivirus envelope and Rev construct (pCMV-VSV-G-RSV-Rev), both of which were provided by Dr. Miyoshi. Then the supernatant containing virus particles was collected, centrifuged, and concentrated 50-fold in volume. The precultured murine BM cells were infected with each retrovirus in the RPMI1641 medium supplemented with the same medium containing protamine sulfate for 48 h in 6-well dishes coated with RetroNectin (Takara Bio Inc., Shiga, Japan).

Colony Assays—Cells were seeded into methylcellulose medium (MethoCult GF M3434; Stem Cell Technologies, Vancouver, Canada) at a density 2.5×10^2 cells/35-mm dish and were cultured with 5% CO_2 at 37 °C. All cultures were performed in triplicate, and the numbers of colonies were counted after 10 days.

In Vitro Immortalization Assays for HPCs—Immortalization assays of HPCs *in vitro* were performed as previously described (34). In brief, 10^4 cells were plated in 1.1 ml of methylcellulose medium (Methocult M3434). After the 1 week of culture, colony numbers were counted, and single-cell suspensions of colonies (10^4 cells) were subsequently replated under identical conditions. Replating was repeated every week in the same way.

Luciferase Assays—Luciferase assays were performed with a dual luciferase reporter system (Promega, Madison, WI), as previously described (35). Briefly, 293T or NIH3T3 cells (2×10^5 cells) were seeded in a 60-mm dish and cultured for 24 h. Using the calcium phosphate coprecipitation method, cells were transfected with 2 μg of reporter gene (pGL3-3×MαP-luciferase, 3×MHC-luciferase, or 1×MPO-luciferase) in combination with 2 μg of pcDNA3-GATA1, pcDNA3-PU.1 (36), or pcDNA3-C/EBPα together with 6 μg of an empty vector or an effector vector for FIP1L1-PDGFRα, H-RasG12V, 1*6-STAT5A (37), or CAAX-p110 (38) and 10 ng of pRL-CMV, a *Renilla* luciferase expression vector. After 12 h, cells were washed, serum-starved for 24 h, and subjected to luciferase assays. After 36 h, the cells were lysed and subjected to a measurement for luciferase activity. The relative firefly luciferase activity was calculated by normalizing transfection efficiency according to the *Renilla* luciferase activity.

Semiquantitative RT-PCR Analysis—Total RNA was isolated from 5×10^4 FACS-sorted GFP-positive cells using TRIzol reagent (Invitrogen). RT-PCR was performed using SuperScript II reverse transcriptase (Invitrogen) according to the manufacturer's instructions. The cDNA product (1 μl) was resuspended in 20 μl of the PCR buffer containing 0.5 units of TaqGold DNA polymerase (PerkinElmer Life Sciences), 2 mM $MgCl_2$, and 15 pmol of forward and reverse primers. The sequences of forward/reverse primer sets were as follows: *C/EBPα*, 5′-GCC TGG CCT TGA CCA AGG AG-3′ and 5′-CAC AGG ACT AGA ACA CCT GC-3′; *GATA-1*, 5′-GGA ATT CGG GCC CCT TGT GAG GCC AGA GAG-3′ and 5′-CGG GGT ACC TCA CGC TCC AGC CAG ATT CGA CCC-3′; *GATA-2*, 5′-CGG AAT TCG ACA CAC CAC CCG ATA CCC ACC TAT-3′ and 5′-CGG AAT TCG CCT ACG CCA TGG CAG TCA CCA TGC T-3′; *IL5-Rα*, 5′-GCC CTT TGA TCA GCT GTT CAG TCC AC-3′ and 5′-CGG AAC CGG TGG AAA CAA CCT GGT C-3′; *MBP*, 5′-ACC TGT CGC TAC CTC CTA-3′ and 5′-GTG GTG GCA GAT GTG TGA-3′; *PU.1*, 5′-GAT GGA GAA AGC CAT AGC GA-3′ and 5′- TTG TGC TTG GAC GAG AAC TG-3′; *HPRT*, 5′-CAC AGG ACT AGA ACA CCT GC-3′ and 5′-GCT GGT GAA AAG GAC CTC T-3′.

The PCR products were electrophoresed in agarose gels containing ethidium bromide, and their amounts were analyzed with a Fluor Imager595 and ImageQuant software (Amersham Biosciences).

Transplantation Assays—Transplantation assays were performed according to procedures described previously (39). Briefly, 8–12-week-old CD45.2 mice were lethally irradiated (900 rads) 24 h before the transplantation. BM cells isolated from congenic C57BL/6 (B6-Ly5.1) mice were transduced with FIP1L1-PDGFRα, and 10,000 GFP-positive cells were injected intravenously in combination with 2×10^5 normal BM cells with CD45.2 phenotype. Chimeric analyses were performed at 4 weeks and 8 weeks, and mice were sacrificed 16 weeks after transplantation. Animal care was performed according to institutional guidelines.

Measurement of Phosphorylation of Intracellular Signaling Molecules—Phosphorylation of intracellular molecules was assessed using Phosflow technology (BD Biosciences) according to the manufacturer's recommendation. Briefly, cells were fixed with Phosflow Fix Buffer and incubated at 37 °C for 10–15 min. After permeabilization at room temperature for 10 min, cells were washed twice with Phosflow Perm/Wash Buffer and incubated at room temperature for 10 min. After the binding reaction to each antibody, cells were washed once with Phosflow Perm/Wash buffer, resuspended in 500 μl of BD Pharmingen stain buffer (BD Bioscience), and then subjected to flow cytometric analysis. All experiments were repeated independently at least three times, and reproducibility was confirmed.

Statistical Analyses—Statistical analyses were performed using Student's *t* test.

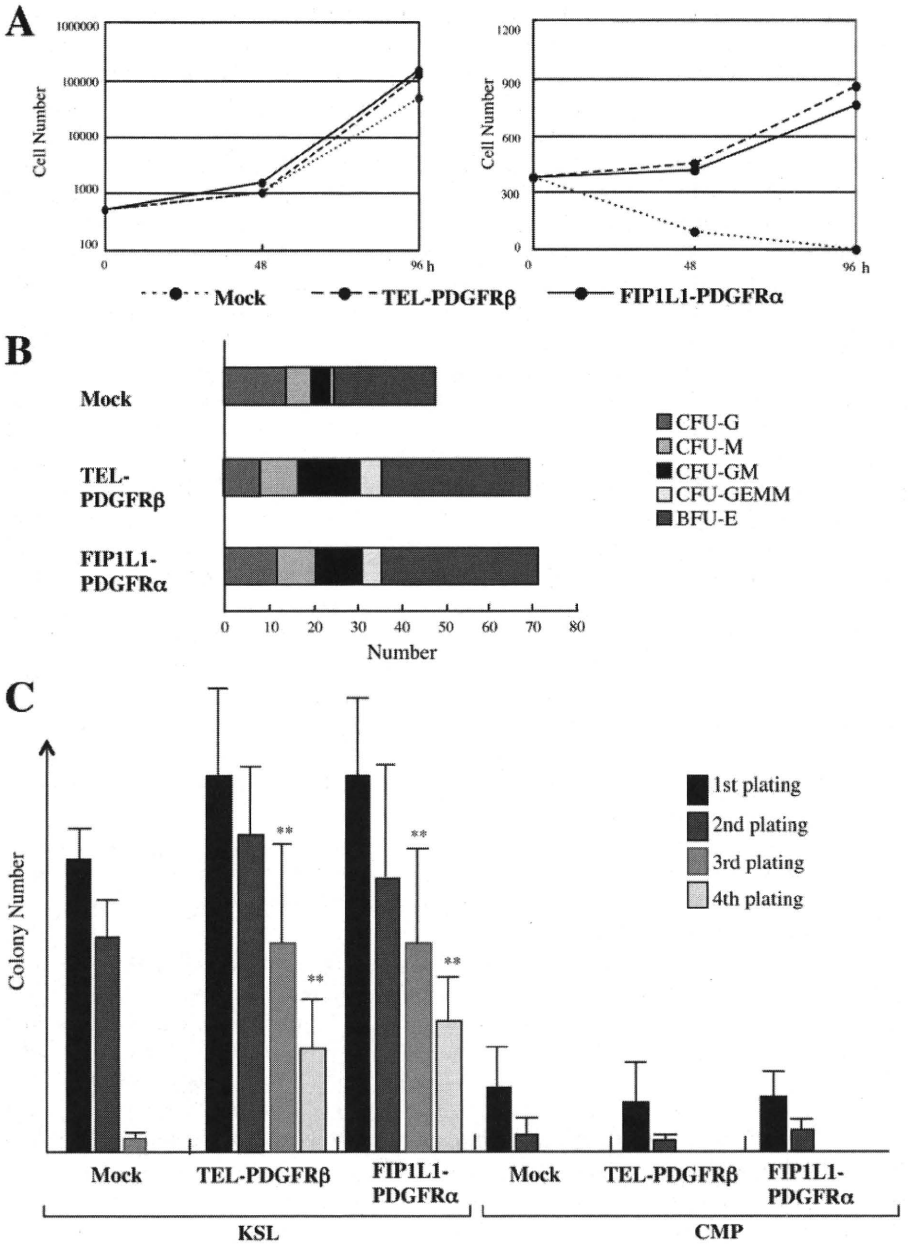

FIGURE 1. **The effects of leukemogenic tyrosine kinases on proliferation and survival of hematopoietic stem/progenitor cells.** *A*, KSLs were isolated from murine bone marrow mononuclear cells. After the retrovirus (mock, FIP1L1-PDGFRα, or TEL-PDGFRβ) infection, retrovirus-infected KSLs were sorted as GFP^+ cells and cultured with (*left*) or without (*right*) SCF, TPO, FLT3L, and IL-6 for 96 h. During these cultures, total viable cell numbers were counted at the time indicated. *B*, KSLs infected with each retrovirus were sorted and seeded into the methylcellulose medium containing EPO, TPO, SCF, granulocyte colony-stimulating factor, and IL-3. Colony numbers were counted on day 12. *C*, immortalization assays for retrovirus-infected KSLs and CMPs. Retrovirus-infected KSLs and CMPs (10^3 cells) were plated into methylcellulose medium, and colony numbers were counted after 1 week. Then single-cell suspensions of colonies (10^3 cells) were serially replated every week in the same way. *Bars*, number of colonies obtained after each round of replating in methylcellulose as means ± S.D. ($n = 3$). **, $p < 0.01$ compared with the value of mock-transduced cells.

RESULTS

Effects of FIP1L1-PDGFRα on the Growth and Survival of Murine KSL Cells—To investigate the effects of LTKs on the growth, differentiation, and survival of HSCs/HPCs, we constructed bicistronic retrovirus vectors for FIP1L1-PDGFRα and TEL-PDGFRβ, which express these cDNAs together with EGFP through the internal ribosome entry site in the infected cells. At first, we introduced these retrovirus vectors into KSL cells. After a 48-h infection, 55–65% of KSLs were found to be GFP-positive in all of transfectants by flow cytometric analysis (data not shown). Next, we isolated retrovirus-infected cells as GFP-positive cells and cultured them in the medium with or without SCF, TPO, FLT3L, and IL-6. As shown in Fig. 1*A* (*left*), neither FIP1L1-PDGFRα nor TEL-PDGFRβ further augmented cytokine-dependent growth of KSLs. However, these LTKs enabled KSLs to survive and proliferate under cytokine-deprived conditions at least for 96 h, whereas mock (an empty retrovirus)-infected KSLs rapidly led to apoptosis in this condition (Fig. 1*A*, *right*).

Next, we performed colony assays using these retrovirus-infected KSLs. After 2-day retrovirus infection, GFP-positive cells were sorted and plated into methylcellulose medium containing the cytokine mixture (EPO, TPO, SCF, granulocyte colony-stimulating factor, and IL-3), and numbers of colonies were counted after 10 days. As shown in Fig. 1*B*, the total number of colonies that developed from FIP1L1-PDGFRα- or TEL-PDGFRβ-infected KSLs was increased by 40–50% as compared with that from mock-infected KSLs. Also, these colonies were larger than those yielded from mock-infected KSLs (data not shown). However, the proportion of CFU-GEMM, CFU-GM, CFU-G, CFU-M, and BFU-E was roughly the same among three transfectants, indicating that these LTKs scarcely influence the lineage commitment and differentiation of KSLs in colony assays performed in this cytokine combination (Fig. 1*B*).

We next performed an *in vitro* immortalization assay using FIP1L1-PDGFRα-, TEL-PDGFRβ-, or mock-transduced KSLs and CMPs. After the first and second plating, both FIP1L1-PDGFRα- and TEL-PDGFRβ-transduced KSLs yielded a slightly increased number of colonies relative to mock-transduced KSLs, whereas these differences were not significant (Fig. 1*C*, *left*). Also, in contrast to mock-transduced KSLs, FIP1L1-PDGFRα- or TEL-PDGFRβ-transduced KSLs

TABLE 1
Peripheral blood examinations 16 weeks after transplantation

Mouse	White blood cells × 10^9/liter	Eosinophil
		%
Mock-1	88.3	1.2
Mock-2	96.2	2.4
Mock-3	83.5	2.6
Mock-4	102.2	0.8
Mock-5	88.2	2
FIP1L1-PDGFRα-1	563.2	3.6
FIP1L1-PDGFRα-2	121.1	1.2
FIP1L1-PDGFRα-3	492.3	4.8
FIP1L1-PDGFRα-4	140.1	3.6
FIP1L1-PDGFRα-5	662.3[a]	0.2

[a] CD3(+)CD8(+) cells: 96%.

still kept colony-forming activities even after the third and fourth plating (FIP1L1-PDGFRα *versus* mock at the third plating, $p < 0.01$; at the fourth plating, $p < 0.01$), although these activities were rather reduced (Fig. 1*C*, *left*). On the other hand, even if FIP1L1-PDGFRα or TEL-PDGFRβ was introduced, CMPs could not form any colony at the third plating, as was the case with mock-infected CMPs (Fig. 1*C*, *right*). To evaluate leukemogenic potential of FIP1L1-PDGFRα-transduced KSLs *in vivo*, we transplanted these cells into lethally irradiated mice in combination with freshly prepared competitor KSLs. As a result, although none of the mice transplanted with mock-transduced KSLs developed leukemia or MPD, FIP1L1-PDGFRα-transduced KSLs developed MPD in three mice and acute leukemia in one mouse of five recipient mice within 15 weeks after transplantation (Table 1). However, in agreement with the previous report (16), none of the five recipient mice developed eosinophilic disorders. In addition, none of the 10 mice transplanted with FIP1L1-PDGFRα-transduced CMPs developed MPD or leukemia (data not shown). Together, these results indicate that FIP1L1-PDGFRα can confer the ability of cytokine-independent growth/survival on KSLs and enhance their self-renewal, whereas it cannot immortalize CMPs *in vitro* or *in vivo*.

Effects of FIP1L1-PDGFRα and TEL-PDGFRβ on Differentiation from KSLs—We next investigated whether FIP1L1-PDGFRα or TEL-PDGFRβ influences the lineage commitment and subsequent differentiation of KSLs. For this purpose, we infected retrovirus harboring FIP1L1-PDGFRα or TEL-PDGFRβ into KSLs; cultured them with SCF, TPO, FLT3L, and IL-6; and examined the expression of a granulocyte marker (Gr-1) and an eosinophil marker (IL-5 receptor α, CD125) in GFP-positive cells by flow cytometry. After 4-day cultures, there was not an apparent difference in the expression pattern of these markers among FIP1L1-PDGFRα-, TEL-PDGFRβ-, and mock-transduced KSLs (Fig. 2*A*, *top*). However, after 6-day cultures, TEL-PDGFRβ- or FIP1L1-PDGFRα-transduced KSLs yielded significantly increased Gr-1^+ fraction (66.8 and 77.5%, respectively) compared with mock-transduced KSLs (49.6%). In addition, it was of particular interest that 51.8% of FIP1L1-PDGFRα-transduced KSLs grew to express CD125 and Gr-1 simultaneously, whereas only 6.0% of mock-transduced and 14.0% of TEL-PDGFRβ-transduced KSLs revealed this phenotype (FIP1L1-PDGFRα *versus* mock, $p < 0.01$; Fig. 2*A*, *bottom*). These results imply that FIP1L1-PDGFRα but not TEL-PDGFRβ preferentially imposes the commitment and differentiation to the eosinophilic lineage.

To examine whether Gr-1^+CD125$^+$ cells that developed from FIP1L1-PDGFRα-transduced KSLs are actually eosinophil precursors, we further cultured these KSLs with a cytokine mixture containing IL-5 for an additional 5 days. As a result, most of FIP1L1-PDGFRα-transduced but not mock- or TEL-PDGFRβ-transduced KSLs came to possess large granule characteristics of mature eosinophil in the MG staining, which were positive for the eosinostain (Fig. 2*B*). Furthermore, after 10-day cultures, we examined the mRNA expression of eosinophil-related genes, *GATA-1*, *IL-5Rα*, and *C/EBPε*, by RT-PCR analysis using sorted GFP-positive cells. As shown in Fig. 2*C*, *IL-5Rα* and *C/EBPε* mRNAs were detected only in FIP1L1-PDGFRα-transduced KSLs. Also, *GATA-1* mRNA was more intensively expressed in FIP1L1-PDGFRα-transduced KSLs than in mock- or TEL-PDGFRβ-transduced KSLs. These data indicate that Gr-1^+CD125$^+$ cells that developed from FIP1L1-PDGFRα-transduced KSLs can indeed differentiate into mature eosinophils.

Effects of FIP1L1-PDGFRα on Differentiation of CMPs, MEPs, and CLPs—It was previously shown that eosinophil precursors stochastically develop from HSCs through MMP, CMP, and GMP (40, 41). Therefore, at first, we examined whether FIP1L1-PDGFRα can enhance the development of eosinophils from CMPs. For this purpose, we isolated CMPs from murine BM mononuclear cells by FACS using several markers (Fig. 3*A*). Then we introduced FIP1L1-PDGFRα into these cells and cultured them with SCF, IL-6, FLT3L, and TPO for 6 days. As was the case with KSLs, FIP1L1-PDGFRα remarkably enhanced the development of Gr-1^+CD125$^+$ cells from CMPs compared with mock cultures (57% *versus* 6%, $p < 0.01$; Fig. 3*B*).

Our next question was whether FIP1L1-PDGFRα could convert the lineages of MEPs and CLPs, which were already committed to the other lineages, into the eosinophil lineage. To address this issue, we introduced FIP1L1-PDGFRα or TEL-PDGFRβ into MEPs. When cocultured with a stroma cell line OP-9 in the presence of SCF and EPO for 9 days, 58% of mock-infected and 41% of TEL-PDGFRβ-infected MEPs came to reveal the Ter119$^+$CD125$^-$ erythroid phenotype. In contrast, only 26% of FIP1L1-PDGFRα-infected MEPs revealed this phenotype (FIP1L1-PDGFRα *versus* mock, $p < 0.05$; Fig. 3*C*, *top*). Moreover, 50% of FIP1L1-PDGFRα-transduced MEPs differentiated into CD125$^+$Gr-1^+ cells, whereas only 16% of mock-infected and 14% of TEL-PDGFRβ-infected MEPs revealed this phenotype (FIP1L1-PDGFRα *versus* mock, $p < 0.01$; Fig. 3*C*, *bottom*). Similarly, after 9-day cultures in serum-free medium supplemented with TPO and IL-11, although mock-transduced MEPs effectively gave rise to CD41$^+$Gr-1^- cells (17%), only 2% of FIP1L1-PDGFRα-infected MEPs revealed this phenotype (FIP1L1-PDGFRα *versus* mock, $p < 0.01$; Fig. 3*D*). Also, mock-transduced MEPs were found to become large polyploid megakaryocytes in morphological analysis, whereas most of the FIP1L1-PDGFRα-transduced MEPs remained small and mononuclear (Fig. 3*E*). Together, these results indicate that FIPIL1-PDGFRα inhibits erythroid and megakaryocytic differentiation from MEPs and imposes lineage conversion to the eosinophil lineage.

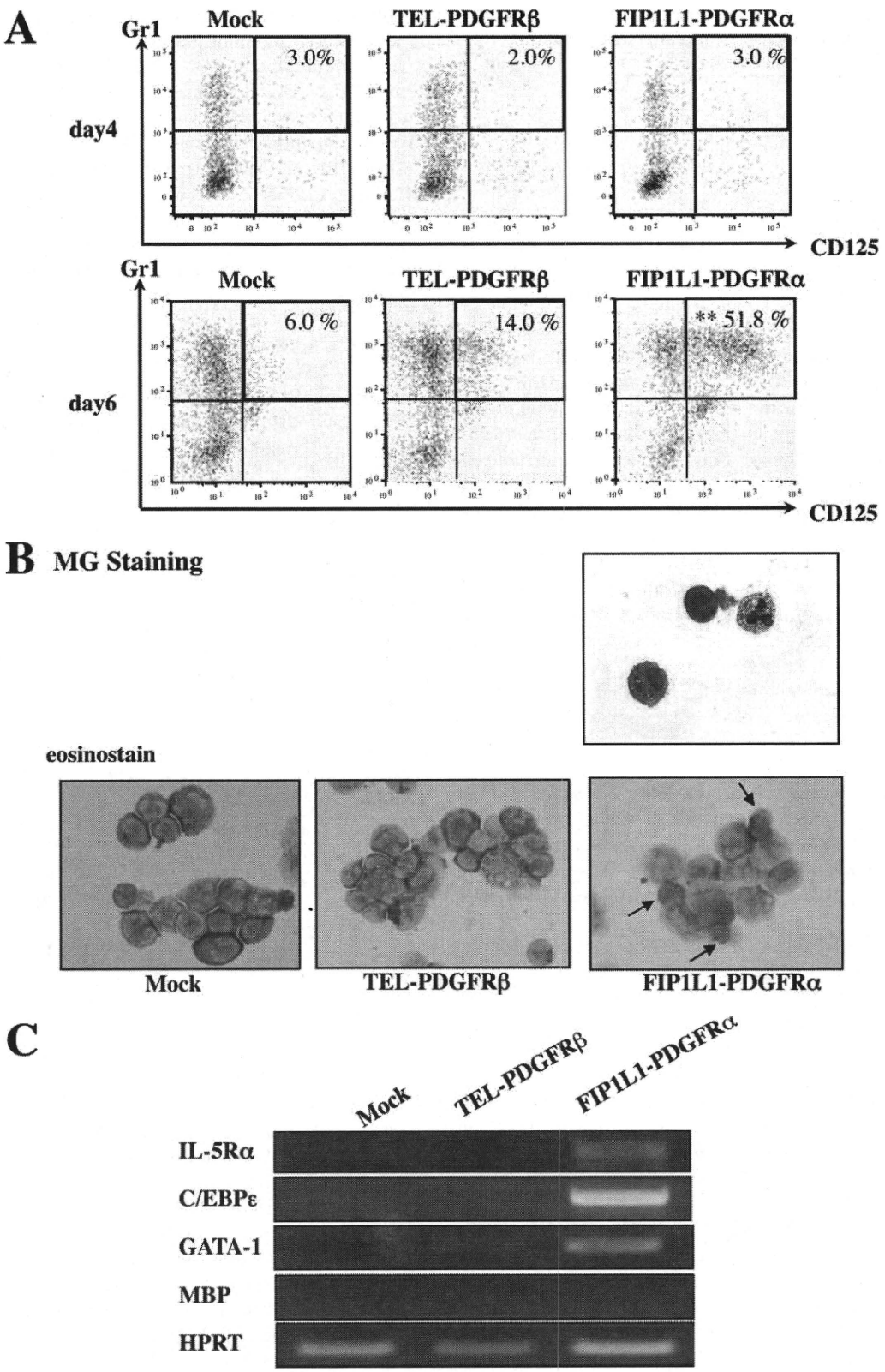

FIGURE 2. **Eosinophil development from KSLs.** *A*, after retrovirus transduction, KSLs were cultured with SCF, TPO, IL-6, and FLT3L, and FACS analysis was performed after 4 days (*top*) and 6 days (*bottom*). GFP^+ cells were gated, and the expression of Gr-1 and CD125 was analyzed. **, $p < 0.01$ compared with the value of mock-transduced cells ($n = 3$). *B*, after 6-day cultures with SCF, TPO, IL-6, and FLT3L, retrovirus-infected KSLs were further cultured with a cytokine mixture containing IL-5 for 5 days. Transduced cells were subjected to May-Giemsa staining (*top*) and eosinostain (*bottom*). *C*, after 10-day cultures with TPO, IL-6, FLT3L, and SCF, GFP-positive cells were sorted, and the expression of eosinophil-related genes was analyzed by RT-PCR analysis.

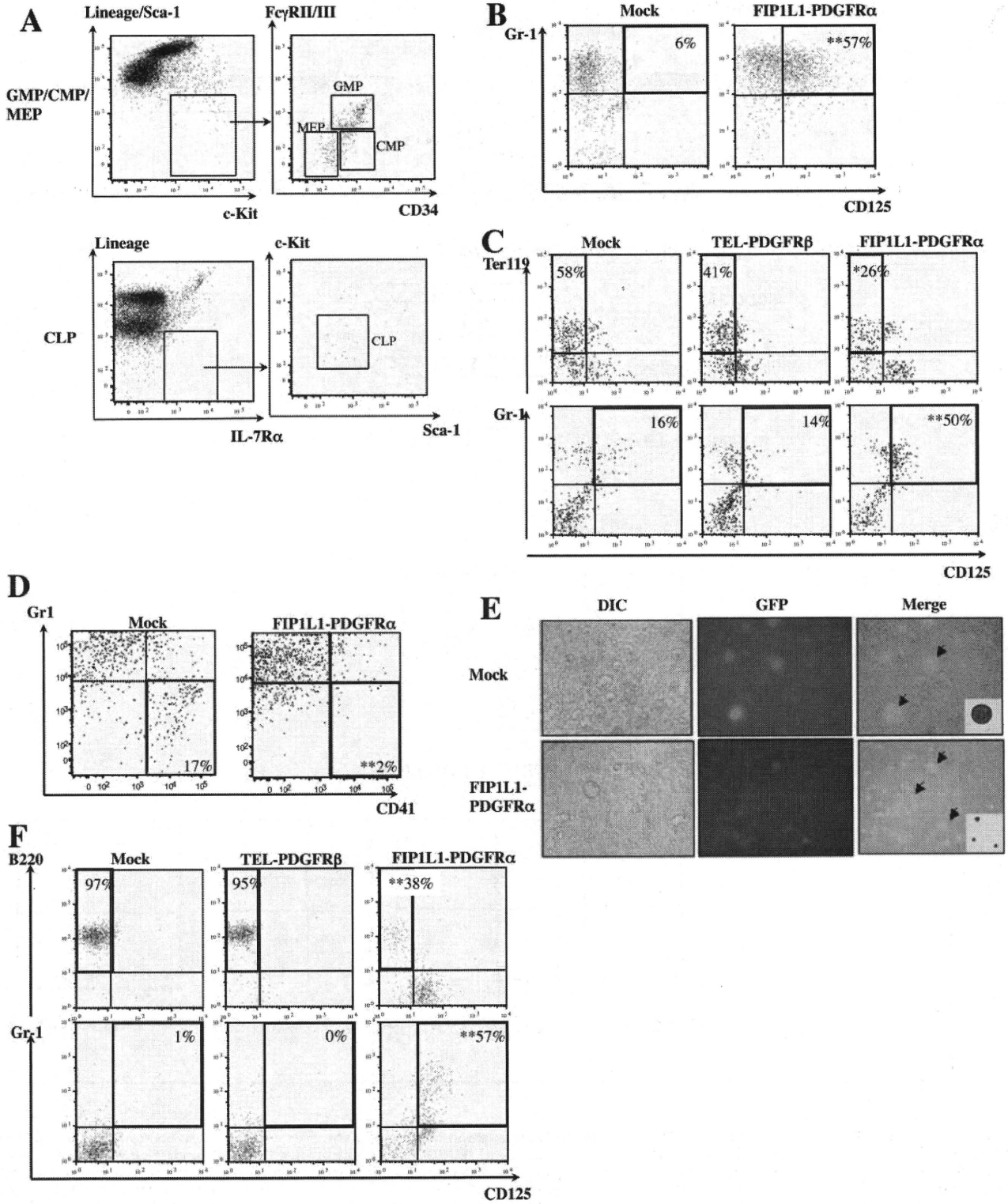

FIGURE 3. **FIP1L1-PDGFRα-induced eosinophil development from CMPs, MEPs, and CLPs.** *A*, isolation of GMPs/CMPs/MEPs and CLPs from murine mononuclear cells by a FACS using several markers. *B*, mock-, FIP1L1-PDGFRα-, or TEL-PDGFRβ-transduced CMPs were cultured with SCF, IL-6, FLT3L, and TPO for 6 days. Then the expression of CD125 and Gr-1 was analyzed by flow cytometry. *C*, mock-, FIP1L1-PDGFRα-, or TEL-PDGFRβ-transduced MEPs were cocultured with OP-9 cells in the presence of EPO and SCF for 8 days and then subjected to FACS analysis. *D* and *E*, mock- or FIP1L1-PDGFRα-transduced MEPs were cultured in serum-free medium supplemented with TPO and IL-11 for 9 days and subjected to FACS analysis. Transduced cells were observed with differential interference contrast (*DIC*) and fluorescence microscopy. Mock- and FIP1L1-PDGFRα-transduced GFP-positive cells (*arrows*) were sorted and subjected to May-Giemsa staining. *F*, retrovirus-transduced CLPs were cocultured with OP-9 cells in the presence of SCF, IL-7, and FLT3L for 2 days. Then granulocyte-macrophage colony-stimulating factor was added into the medium, and cells were cultured for an additional 8 days. **, $p < 0.01$ compared with the value of mock-transduced cells ($n = 3$).

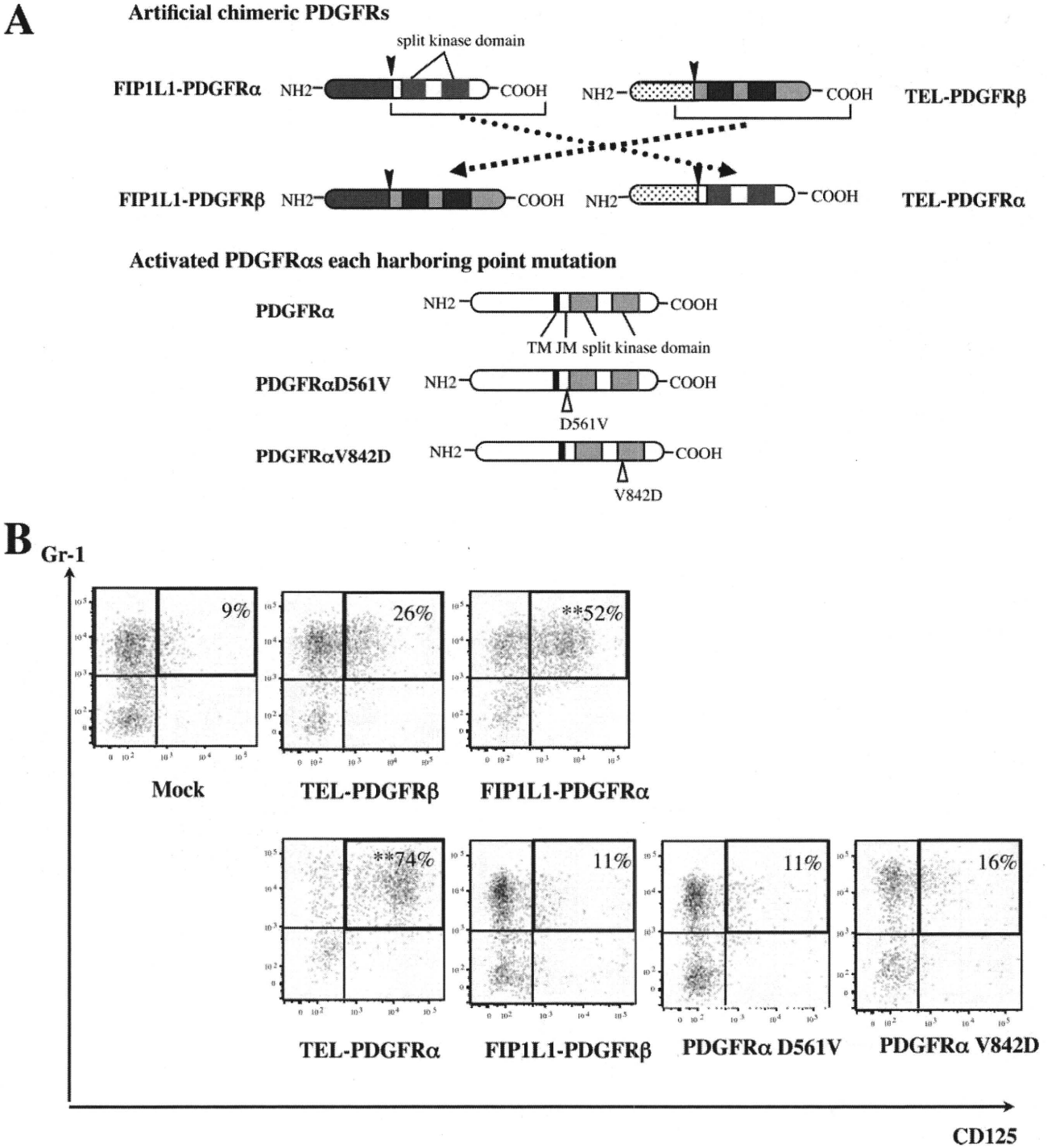

FIGURE 4. **Function of FIP1L1 and PDGFRα in FIP1L1-PDGFRα-induced eosinophil development.** *A*, schematic representation of FIP1L1-PDGFRβ and TEL-PDGFRα, PDGFRαD561V, and PDGFRαD842V. In FIP1L1-PDGFRβ and TEL-PDGFRα, FIP1L1 in FIP1L1-PDGFRα and TEL in TEL-PDGFRβ were completely exchanged one another. Splicing sites are indicated with *black arrows*, and point mutation sites are indicated with *vacant arrows*. *TM*, transmembrane domain; *JM*, juxtamembrane domain. *B*, murine KSLs were infected with the retrovirus, as indicated, and cultured with SCF, TPO, IL-6, and FLT3L for 6 days. Then expression of CD125 and Gr-1 was analyzed by flow cytometry. **, $p < 0.01$ compared with the value of mock-transduced cells ($n = 3$).

Next, we introduced FIP1L1-PDGFRα into CLPs and cocultured them with OP-9 cells in the presence of SCF, IL-7, and FLT3L. After 10-day cultures, 97% of mock- and 95% of TEL-PDGFRβ-transduced CLPs came to have the $B220^+CD125^-$ B-lymphoid phenotype, whereas only 38% of FIP1L1-PDGFRα-transduced CLPs had this phenotype (FIP1L1-PDGFRα *versus* mock, $p < 0.01$). Furthermore, a considerable proportion of FIP1L1-PDGFRα-transduced CLPs but